Journal of Medicinal Chemistry

Article

Discovery and in Vivo Evaluation of the Potent and Selective PI3K# Inhibitors 2-((1S)-1-((6-Amino-5-cyano-4-pyrimidinyl)amino)ethyl)-6-fluoro-N-methyl-3-(2-pyridinyl)-4-quinolinecarboxamide (AM-0687) and 2-((1S)-1-((6-Amino-5-cyano-4-pyrimidinyl)amino)ethyl)-5-fluoro-N-methyl-3-(2-pyridinyl)-4-quinolinecarboxamide (AM-1430)

Felix Gonzalez-Lopez de Turiso, Xiaolin Hao, Youngsook Shin, Minna Bui, Iain David Grant Campuzano, Mario G. Cardozo, Michelle C. Dunn, Jason Duquette, Benjamin Fisher, Robert S. Foti, Kirk R Henne, Xiao He, Yi-Ling Hu, Ron C. Kelly, Michael G Johnson, Brian S Lucas, John D McCarter, Lawrence R McGee, Julio C Medina, Daniela P. Metz, Tisha San Miguel, Deanna Mohn, Thuy Tran, Christine Vissinga, Sharon Wannberg, Douglas A. Whittington, John Whoriskey, Gang Yu, Leeanne Zalameda, Xuxia Zhang, and Timothy D. Cushing

J. Med. Chem., **Just Accepted Manuscript** • DOI: 10.1021/acs.jmedchem.6b00827 • Publication Date (Web): 14 Jul 2016

Just Accepted

ACS Publications

Journal of Medicinal Chemistry is published by the American Chemical Society. 1155 Sixteenth Street N.W., Washington, DC 20036

Discovery and in Vivo Evaluation of the Potent and Selective PI3Kδ Inhibitors 2-((1*S*)-1-((6-Amino-5-cyano-4-pyrimidinyl)amino)ethyl)-6-fluoro-N-methyl-3-(2-pyridinyl)-4-quinolinecarboxamide (AM-0687) and 2-((1*S*)-1-((6-Amino-5-cyano-4-pyrimidinyl)amino)ethyl)-5-fluoro-*N*-methyl-3-(2-pyridinyl)-4-quinolinecarboxamide (AM-1430)

Felix Gonzalez-Lopez de Turiso,[‖,*] *Xiaolin Hao,*[†] *Youngsook Shin,*[‡,*] *Minna Bui,*[†] *Iain D. G. Campuzano,*[‡] *Mario Cardozo,*[†] *Michelle C. Dunn,*[†] *Jason Duquette,*[†] *Benjamin Fisher,*[†] *Robert S. Foti,*[‖] *Kirk Henne,*[§] *Xiao He,*[†] *Yi-Ling Hu,*[#] *Ron C. Kelly,*[⊥] *Michael G. Johnson,*[†] *Brian S. Lucas,*[†] *John McCarter,*[‡] *Lawrence R. McGee,*[†] *Julio C. Medina,*[†] *Daniela Metz,*[#] *Tisha San Miguel,*[‡] [#]*Deanna Mohn,* [#] *Thuy Tran,*[§] *Christine Vissinga,*[#] *Sharon Wannberg,*[#] *Douglas A. Whittington,*[I] *John Whoriskey,*[#] *Gang Yu,* [#] *Leeanne Zalameda,*[‡] *Xuxia Zhang,* [#] *Timothy D. Cushing.*[†]

[†]Department of Therapeutic Discovery, [§]Department of Pharmacokinetics and Drug Metabolism, Amgen Inc., 1120 Veterans Boulevard, South San Francisco, California 94080, United States.

[‡]Department of Therapeutic Discovery, [#]Department of Inflammation Research, [⊥]Drug Product Technologies, Amgen Inc., One Amgen Center Drive, Thousand Oaks, California 91320, United States.

[∥]Department of Therapeutic Discovery, [∥∥]Department of Pharmacokinetics and Drug Metabolism, Amgen Inc., 360 Binney Street, Cambridge, Massachusetts 02142, United States.

ABSTRACT

Optimization of the potency and pharmacokinetic profile of 2,3,4-trisubstituted quinoline **4**, led to the discovery of two potent, selective, and orally bioavailable PI3Kδ inhibitors, **6a** (AM-0687) and **7** (AM-1430). On the basis of their improved profile, these analogs were selected for in vivo pharmacodynamic (PD) and efficacy experiments in animal models of inflammation. The in vivo PD studies, which were carried out in a mouse pAKT inhibition animal model, confirmed the observed potency of **6a** and **7** in biochemical and cellular assays. Efficacy experiments in a keyhole limpet hemocyanin (KLH) model in rats demonstrated that administration of either **6s** or **7** resulted in a strong dose-dependent reduction of IgG and IgM specific antibodies. The excellent in vitro and in vivo profiles of these analogs make them suitable for further development.

INTRODUCTION

Phosphoinositide 3-kinases (PI3Ks) are lipid kinases that phosphorylate the 3′ position of the inositol ring in phosphatidylinositol.[1] The resulting phosphoinositides (PIs) are secondary messengers that play central roles in the regulation of cellular processes including signal transduction, cell survival and control of membrane trafficking. Thus, inhibition of PI3K activity has been regarded as a suitable strategy to modulate these key cellular processes.[2,3]

Among the different types of PI3Ks, class I PI3Ks play a central role in the regulation of phosphatidylinositol (3,4,5)-triphosphate (PIP3) levels. Importantly, PIP3 functions as a membrane anchoring site for key protein kinases including serine/threonine kinases such as AKT (or PKB), PDK1 and tyrosine kinases of the Tec family. Regulation of the PIP3 level in the cell is controlled by two different subclasses of class I PI3Ks: class IA, which is comprised of PI3Kα, β and δ isoforms and class IB, which is comprised of PI3Kγ.[4,5] In terms of tissue distribution, PI3Kα and PI3Kβ are ubiquitously expressed whereas PI3Kγ and PI3Kδ are primarily found in leukocytes.[6] The key role of class I PI3Ks in signal transduction in combination with its tissue distribution and mouse genetic studies have made small molecule inhibition of class I PI3Ks a prominent area of research within the pharmaceutical industry.[7,8] Despite this interest, only one PI3Kδ inhibitor (Idelalisib) has been approved for the treatment of certain types of cancer. The limited success in this field is a testimony to not only the vast amount of research necessary to bring a new medicine to patients, but also the importance of flexibility during clinical trial design and execution. In particular, within the PI3K field, mouse genetic studies and preclinical animal models of disease established PI3Kα and PI3Kβ as plausible targets for the treatment of human cancer[8] whereas PI3Kγ and PI3Kδ, which have a central role in leukocyte biology, were viewed as attractive targets for the treatment of inflammatory diseases.[9] Despite this data, clinical trials in cancer patients with PI3Kα and PI3Kβ inhibitors are still in progress and results from pivotal Phase 2 and Phase 3 clinical trials for drug approval are still pending.[10] Concurrent with these studies, the realization that PI3K mediated human B cell modulation could be beneficial for the treatment of certain types of leukemias led to the repositioning of PI3Kδ inhibitors as potential therapeutics for the treatment of oncologic diseases.[11] This change in development strategy proved critical for the successful outcome of the PI3Kδ field and has resulted in the accelerated approval of Idelalisib for the treatment of patients suffering from relapsed chronic lymphocytic leukemia (in combination with Rituximab),[12] relapsed follicular non-Hodgkin lymphoma and relapsed small lymphocytic lymphoma.[13]

Our own research efforts in this field have focused on a rational design approach to identify PI3K inhibitors with built in kinase and isoform selectivity for the treatment of both oncologic and inflammatory human diseases. Some of the initial work in this area described the identification and in vivo evaluation of PI3Kα, dual PI3Kβ/δ and selective PI3Kδ inhibitors (Figures 1a and 1b).[14] Recently, the identification of the clinical candidate **3** (AMG 319), which is currently being evaluated in Phase 2 clinical trials for the treatment of human papillomavirus (HPV) and negative head and neck squamous cell carcinoma (HNSCC) has also been reported.[15] Herein we describe the discovery and in vivo preclinical studies of **6a** and **7**, two potent and selective PI3Kδ inhibitors containing a unique 4-carboxamide quinoline pharmacophore. These studies are part of an effort to identify a clinical candidate with suitable profile for the treatment of inflammatory diseases.

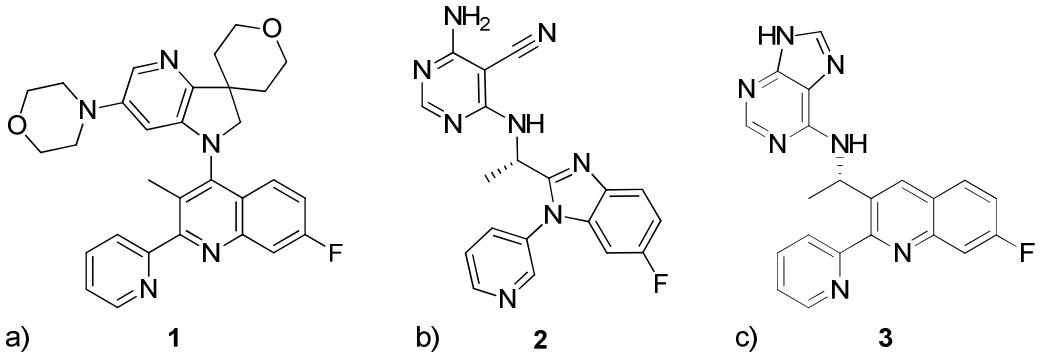

Figure 1. Structures of PI3K inhibitors. a) Dual PI3Kβ/δ inhibitor, b) Selective PI3Kδ inhibitor, c) Selective PI3Kδ inhibitor.

RESULTS AND DISCUSSION

Optimization Strategy

Efforts to identify a second clinical candidate within the PI3Kδ program focused on further improving the isoform selectivity profile of **3** while maintaining its favorable PK parameters. A number of different strategies were pursued to achieve this goal, including exploration of new chemical series (e.g., benzimidazoles,[14a]

naphthyridines,[16] pyridopyrimidinones[17] or thienopyridines[18]) as well as small modifications of the quinoline ring present in the **3** series (Figure 2).[19] The latter approach led to the identification of the 2,3,4-substituted quinoline pharmacophore exemplified by **4**, a reasonably potent and selective PI3Kδ inhibitor.[20] At the outset, this compound was viewed as a suitable lead for further optimization and work focused on improving its intrinsic microsomal stability and PXR activation profile (Figure 2). To address these issues the strategy focused on reducing the clogP of these analogues by replacing the pyridine ring at C4 with more polar groups.

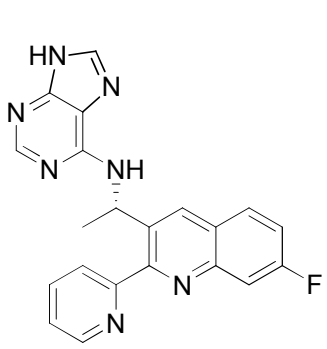

3

PI3Kα[a] IC_{50} = 33000 nM
PI3Kβ[a] IC_{50} = 2700 nM
PI3Kδ[a] IC_{50} = 18 nM
PI3Kγ[a] IC_{50} = 850 nM

pAKT[b] IC_{50} = 1.5 nM

HLM[c] Cl_{int} = <14 μL/min·mg
hPXR[d] POC @ 2,10 μM = 3, 8%

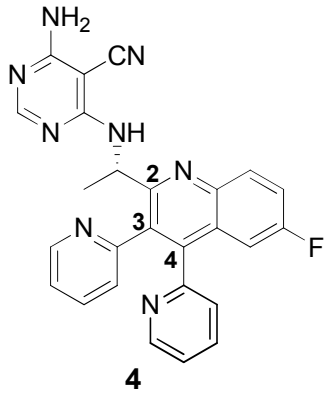

4

PI3Kα[a] IC_{50} = 7900 nM
PI3Kβ[a] IC_{50} = 2800 nM
PI3Kδ[a] IC_{50} = 2.4 nM
PI3Kγ[a] IC_{50} = 850 nM

pAKT[b] IC_{50} = 8.6 nM

HLM[c] Cl_{int} = 47 μL/min·mg
hPXR[d] POC @ 2,10 μM = 8, 51%

Figure 2. Profile of PI3Kδ inhibitors **3** and lead compound **4**. [a]Biochemical: Alphascreen assay. [b]Cellular: In vitro HTRF assay, phosphorylated-AKT.[c]Single experimental values. %Turnover was measured by LC/MS after incubation of parent compound (1 μM) in liver microsome (0.25 mg/mL) in potassium phosphate (66.7 mM) buffered with NADPH (1 mM) at 37 °C for 30 min. [d]human Pregnane X Receptor. Data are shown as Percent of Control.

Due to the synthetic accessibility of a C3 phenyl-substituted quinoline penultimate intermediate (carboxylic acid **15**, Scheme 1), initial optimization of the C4 group was performed within this series. Preliminary work focused on replacing the pyridine ring at C4 with small functional groups that would also contain a H-bond acceptor (Figure 3a, general structure **5**).[21] After a suitable replacement of the pyridine ring was identified, our

attention was refocused on improvement of the PXR activation profile by further reducing clogP. Among the compounds synthesized, the series in which the C3 pyridine substituent had been reintroduced was found to display the best overall profile (Figure 3b, general structure **6**). Finally, modification of the 6-F-quinoline substitution pattern was also explored since previous optimization of the **3** series suggested that this modification could improve the overall profile of these inhibitors (Figure 3c, representative structure **7**).[15]

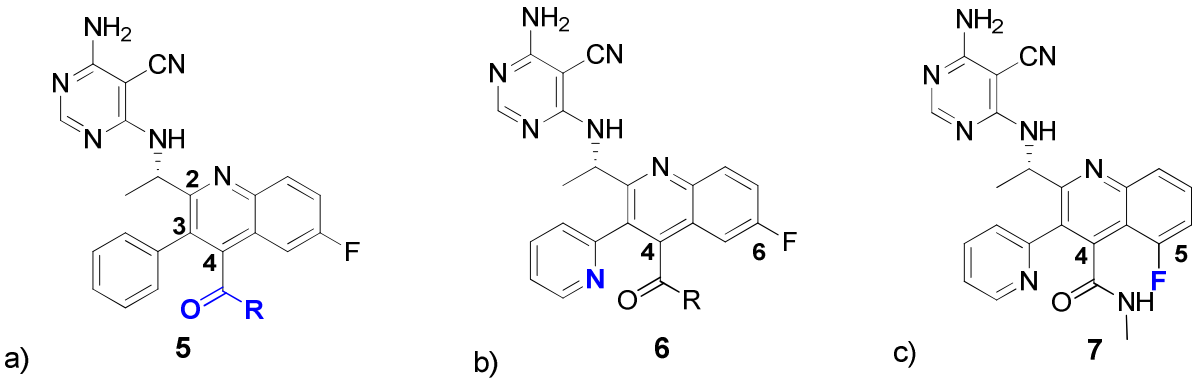

Figure 3. Strategy for optimization of quinoline analogs. a) Introduction of a small, polar group with a H-bond acceptor at C4. b) Introduction of a pyridine ring to reduce clogP. c) Introduction of a 5-F-substituted quinoline.

Chemistry

With this strategy in mind, a rapid synthesis of 3-phenylquinoline derivatives was developed (Scheme 1). Pfitzinger condensation between 5-fluoroisatin (**8**) and 1-phenylbutan-2-one provided 4-quinoline acid **9**.[22] Next, exposure of **9** to thionyl chloride followed by a methanol quench afforded methyl ester **10**. Treatment of **10** with 1,3-dibromo-5,5-dimethylhydantoin in the presence of a radical initiator provided benzyl bromide **11**, which was converted to the corresponding amine intermediate **12** in two steps including: 1) substitution using sodium azide and 2) hydrogenation under Pd/C catalysis. Key carboxylic acid **14** was obtained through a S_NAr reaction between **12** and 4-amino-6-chloropyrimidine-5-carbonitrile followed by LiI-mediated methyl ester hydrolysis. Chiral acid **15** was obtained by SFC purification of this racemate (using isopropanol/hexane

gradient on an AD column) and the final analogs **5a-c** and **5f-i** were synthesized through treatment of **15** with various amines and the coupling reagent PyBop in DMF.

The synthesis of analogs **5d** and **5e** began with the Boc-protection of racemic amine **12**. The resultant intermediate was purified by chiral SFC to afford chiral carbamate **16**. The methyl ester substituent of **16** was then hydrolyzed under aqueous basic conditions to give the corresponding acid, which was subsequently coupled with either ethylamine or isopropylamine to provide **17d** and **17e**, respectively. The final analogs **5d** and **5e** were obtained after HCl-mediated Boc-deprotection and S_NAr of the corresponding amines with 4-amino-6-chloropyrimidine-5-carbonitrile.

Scheme 1[a]

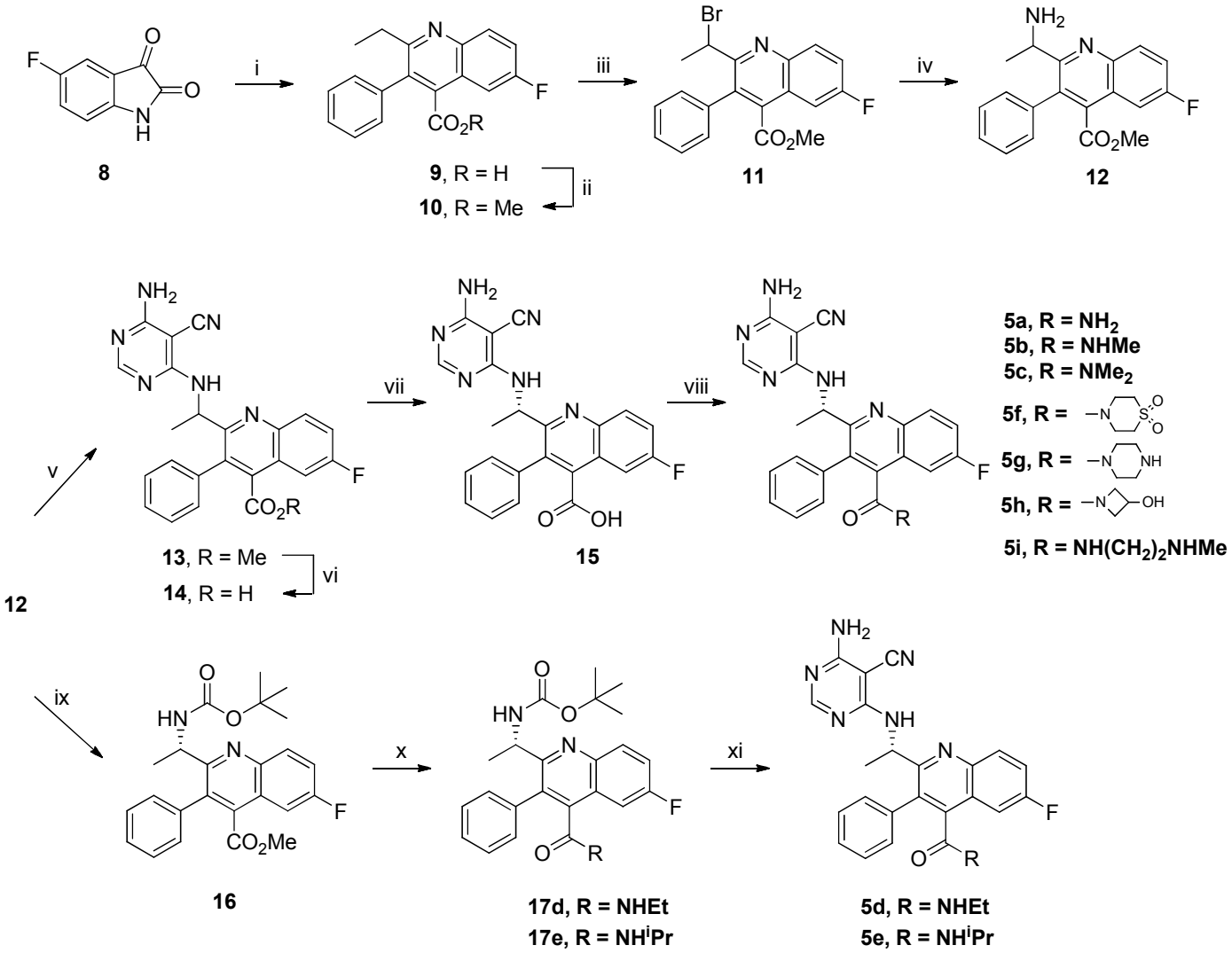

[a] Reagents and conditions: (i) 1-phenylbutan-2-one, KOH, EtOH, reflux, 96%; (ii) $SOCl_2$, MeOH, 21%; (iii) 1,3-dibromo-5,5-dimethylhydantoin, benzoyl peroxide (cat.), CCl_4, reflux, 56%; (iv) 1. NaN_3, DMF; 2. H_2, Pd/C, MeOH, 95% over two steps; (v) 4-amino-6-chloropyrimidine-5-carbonitrile, *n*-BuOH, Hunig's base, 110 °C; (vi) LiI, pyridine, 100 °C, 81% over two steps; (vii) chiral separation, 45%; (viii) amine, PyBop, Hunig's base, DMF, 13-99%; (ix) 1. Boc_2O, TEA, THF, r.t., 77%; 2. chiral separation, 44%; (x) 1. NaOH, MeOH, 60 °C, 99%; 2. amine, PyBop, Hunig's base, DMF, 69-86%; (xi) 1. HCl, r.t.; 2. 4-amino-6-chloropyrimidine-5-carbonitrile, *n*-BuOH, Hunig's base, 100 °C, 31-68% over 2 steps.

The synthesis of the C3 pyridine compounds was performed following two different routes (Schemes 2 and 3). Analog **6d** was synthesized following a synthetic route similar to that described in Scheme 1 (albeit in lower yield). The methyl ester **19** was obtained by Pfitzinger condensation of **8** with 1-(pyridin-2-yl)butan-2-one and subsequent esterification with $TMSCHN_2$. An analogous three step benzylic amination procedure was followed, which included: 1) bromination, 2) substitution, and 3) azide reduction to yield amine **21**. Coupling

of this intermediate with 4-amino-6-chloropyrimidine-5-carbonitrile and hydrolysis of the resultant methyl ester provided acid **23**. Finally, the analog **6d** was obtained via PyBop-mediated amide coupling with azetidin-3-ol as a racemate.

Scheme 2[a]

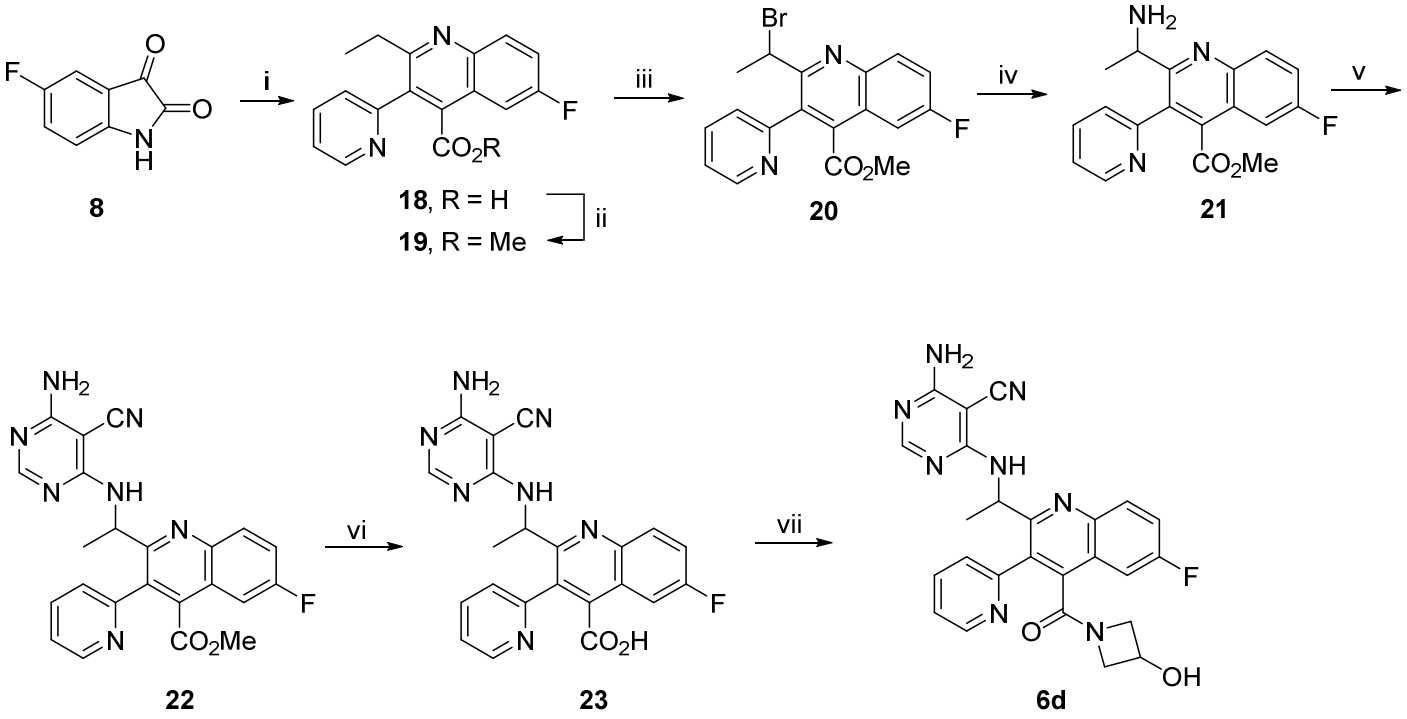

[a]Reagents and conditions: (i) 1-(pyridin-2-yl)butan-2-one, KOH, EtOH, reflux, 99%; (ii) $TMSCHN_2$, MeOH, r.t., 29%; (iii) 1,3-dibromo-5,5-dimethylhydantoin, benzoyl peroxide (cat.), CCl_4, reflux, 80%; (iv) 1. NaN_3, DMF; 2. H_2, Pd/C, 86% over two steps; (v) 4-amino-6-chloropyrimidine-5-carbonitrile, *n*-BuOH, Hunig's base, 100 °C, 98%; (vi) LiI, pyridine, 100 °C, 98%; (vii) amine, PyBop, Hunig's base, DMF, 13%.

The low yield of the previous route prompted the development of an alternative approach for the synthesis of analogs **6a,b** and **6e** (Scheme 3). This route commenced with known ketone **24** (prepared in one step from the corresponding Weinreb amide), which when refluxed with 5-fluoroisatin **8** and potassium hydroxide in ethanol gave acid **25**. This intermediate was then coupled to a variety of different amines under the previously described PyBop conditions to deliver the corresponding amides **26a,b** and **26e**. Amides **26a**,**b** and **26e** were

then treated with 4 N HCl to remove the Boc protecting group. Subsequent S_NAr reaction of the crude amine with 4-amino-6-chloropyrimidine-5-carbonitrile provided the final products **6a**, **6b** and **6e** after chiral separation (Scheme 3-top). The synthesis of **6c** (Scheme 3-bottom) began with the coupling of key acid intermediate **25** with benzyl piperazine-1-carboxylate under standard conditions. Deprotection of the Boc-group and a S_NAr reaction of the resultant amine with 4-amino-6-chloropyrimidine-5-carbonitrile afforded **27**. Final deprotection of the Cbz group in **27** provided analog **6c**.

Scheme 3[a]

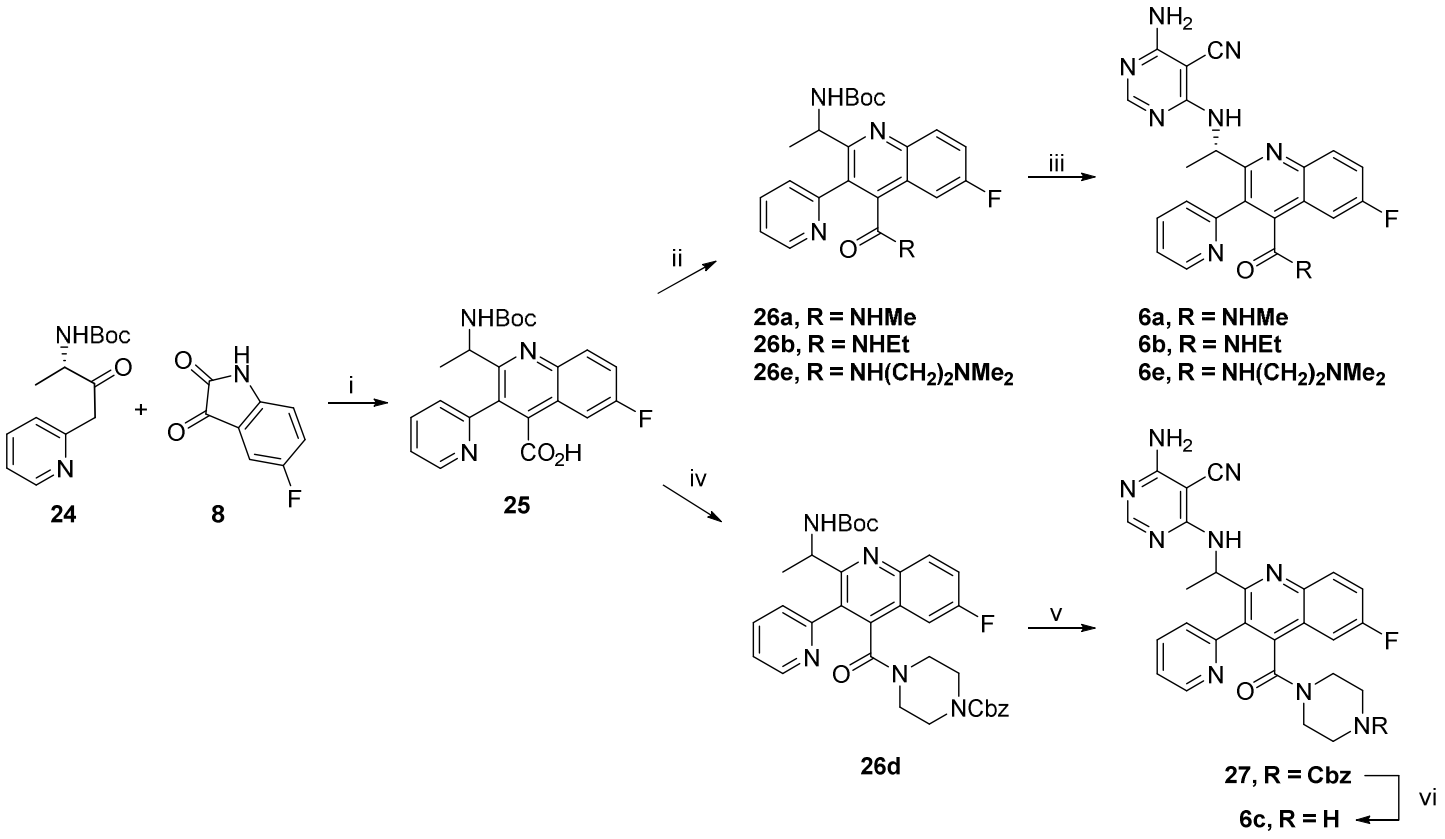

[a]Reagents and conditions: (i) **8**, KOH, EtOH, reflux, 78%; (ii) R^1R^2NH, PyBop, Hunig's base, DMF, 75%; (iii) 1. 4N HCl in dioxane; 2. *n*-BuOH, Hunig's base, 4-amino-6-chloropyrimidine-5-carbonitrile, 110 °C; c) chiral separation, 13-42% from **26a,b,e**; iv) amine, PyBop, Hunig's base, DMF, 24%; v) 1. 4N HCl in dioxane; 2. *n*-BuOH, Hunig's base, 4-amino-6-chloropyrimidine-5-carbonitrile, 110 °C, 100%; (vi) H_2, 10% Pd/C, MeOH, 26%.

An analogous synthetic route to that described in Scheme 3 enabled the synthesis of the 5-fluoro analog **7**. This sequence started with commercially available 4-fluoroisatin and *N*-Boc-protected ketoamino intermediate **24**,

which provided acid intermediate **28** via the previously described Pfitzinger condensation (Scheme 4). Coupling of intermediate **28** with methylamine using PyBop and Hunig's base provided Boc-protected intermediate **29**. Deprotection of the Boc-group with 4N HCl in dioxane and subsequent S_NAr reaction of the amino intermediate with 4-amino-6-chloropyrimidine-5-carbonitrile provided the desired racemic **7**. Chiral separation by SFC led to the isolation of **7**.

Scheme 4[a]

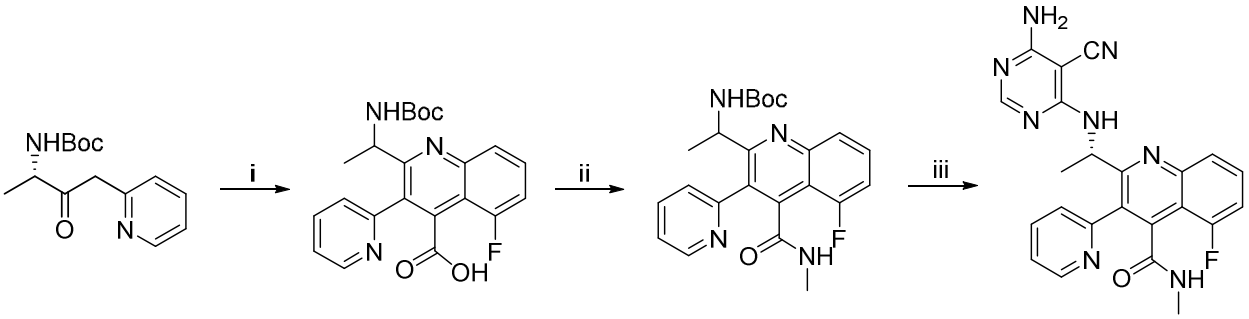

24 **28** **29** **7**

[a]Reagents and conditions: (i) 4-fluoroisatin, KOH, EtOH, reflux, 72%; (ii) $MeNH_2$, PyBop, Hunig's base, DMF, 86%;

(iii) a) 4N HCl in dioxane; b) 1. *n*-BuOH, Hunig's base, 4-amino-6-chloropyrimidine-5-carbonitrile, 110 °C; 2. chiral separation, 13% from **29**.

Structure Activity Relationship (SAR)

Initial replacement of the pyridine ring at the C4 position in **4** with a primary amide led to an improvement in both biochemical and cellular potencies (**5a**, Table 1). This analog also displayed improved in vitro microsomal stability and PXR activation profile relative to the parent bis-pyridine compound **4**. A further improvement in biochemical and cellular potency was achieved by replacing the primary amide in **5a** with a methylamide (**5b**, Table 1). Compound **5b** also had improved PI3Kα/γ isoform selectivity relative to **5a**. The low microsomal intrinsic clearance correlated well with a favorable PK profile (Cl = 0.5 L/hr/kg) and the Clu (clearance corrected by free fraction) was comparable to that observed in **3** (4.5 vs 2.7 L/hr/kg, Table 1).[23] Introduction of

a dimethylamide at the C4 position (analog **5c**, Table 1) led to a marginal improvement in biochemical potency, but the PXR activation profile was unfavorable (75 and 151 POC at 2 and 10 μM, respectively). The secondary ethylamide substitution (analog **5d**, Table 1) was significantly less potent that the corresponding methylamide **5b** (51 vs 1.3 nM) in the biochemical assay. Cyclic tertiary amides were also evaluated (analogs **5f**, **5g**, **5h**, Table 1). Among these, the piperazine amide **5g** displayed the most favorable potency profile (0.2 nM against PI3Kδ in the biochemical assay), but the rat PK was significantly worse (Clu = 60 L/hr/kg).

Table 1: SAR of 3-phenyl analogs **5a-i**.

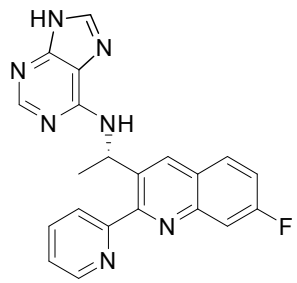

3

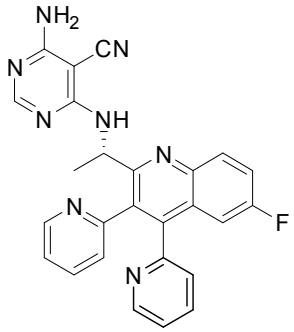

4

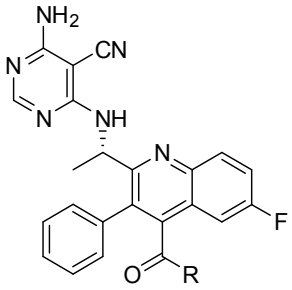

5a-h

Cmpd	R	Biochemical potency[a] PI3K IC_{50} (nM)				Cellular potency		ADME Properties				Calculated properties
						Human B cell[b]	Mouse B cell (pAKT)[c]	RLM / HLM[d]	CYP3A4 / 2D6[e]	hPXR[f]	Cl / Clu[g]	clogP / LipE
		δ	α	β	γ	IC_{50} (nM)	IC_{50} (nM)	μL/(min·mg)	IC_{50} (μM)	POC @ 2/10 μM	L/hr/kg	
3	-	18	33000	2700	850	8.6	1.5	<14 / <14	>27 / >27	3 / 8	0.3/2.7	2.3 / 4.9
4	-	2.8	7900	2800	850	4.6	8.6	16 / 47	>27 / >27	8 / 51	-	2.3 / 6.6
5a	$–NH_2$	2	5760	3540	301	1.8	-	<14 / <14	13 / >27	5 / 33	0.6/-	2.1 / 6.8
5b	–NHMe	1.3	12600	1240	634	1.9	0.3	15 / <14	14 / >27	15 / 52	0.5/4.5	2.5 / 7.1
5c	$–NMe_2$	0.8	703	545	146	2.2	-	426 / 198	19 / >27	75 / 151	-	2.3 / 7.7
5d	–NHEt	51	6230	17000	4650	1.2	-	<14 / 22	>27 / >27	4 / 61	-	3.0 / 4.6
5e[h]	$–NH^iPr$	3.2	12700	8050	853	1.3	-	<14 / 51	13 / >27	38 / 128	-	3.3 / 5.5
5f	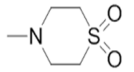	1.2	444	143	35.4	-	-	78 / 62	>27 / >27	50 / 63	-	1.5 / 6.7
5g	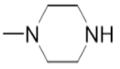	0.2	949	1100	22.5	1.2	-	50 / 82	>27 / >27	7.4 / -	0.9/60	2.4 / 7.5

5h	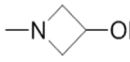	1.3	-	2720	507	-	-	49 / 40	>27 / >27	3.3 / 17	-	2.3 / 6.8
5i	–NH(CH$_2$)$_2$NHMe	9.5	-	15300	9550	2.9	-	<14 / <14	>27 / >27	-4.1 / 5.6		2.3 / 5.7

[a]Biochemical: Alphascreen assay. [b]Cellular: In vitro anti-IgM/CD40L-induced human B cell proliferation (as measured by thymidine incorporation) assay. [c]Cellular: Ability of compound to inhibit anti-IgM induced AKT phosphorylation (pAKT^{Ser473}) in mouse B cells; phospho-AKT (pAKT) expression on B220+gated B cells was determined by flow cytometry in mouse splenocytes. [d]Single experimental values. % Turnover was measured by LC/MS after incubation of parent compound (1 μM) in liver microsome (0.25 mg/mL) in potassium phosphate (66.7 mM) buffered with NADPH (1 mM) at 37 ºC for 30 min. [e]CYP: cytochrome P450 assay competitive (midazolam as probe substrate, 5 μM) reported as % inhibition at 3 μM (LC/MS); [f]human Pregnane X Receptor. Data are shown as Percent of Control. [g]PK experiments were carried out using male Sprague-Dawley rats (n=3). Test compounds formulated at appropriate concentrations for either IV (0.5 mL/kg) or oral (2-10 mL/kg) administration. Unbound clearance equals the total clearance divided by the rat fraction unbound ($CL_u = CL/f_u$). [h]Racemic compound.

With the goal of improving the unfavorable PXR activation profile observed in some of the most promising analogs (e.g., **5a-c**), a strategy directed towards introducing polarity in **5a-h** was pursued. Consistent with the structure of bis-pyridine analog **4**, it was predicted that replacement of the phenyl group at C3 in analogs **5a-h** with a pyridine ring would not be detrimental to potency and could potentially address the PXR activation liability. To test this hypothesis analogs **6a-e**, and **7** were synthesized.

Table 2: SAR of analogs **6a-e** and **7**.

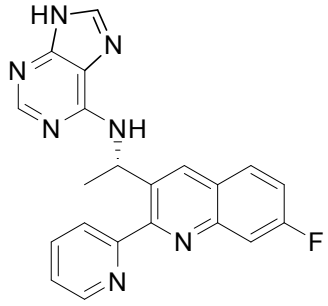

3

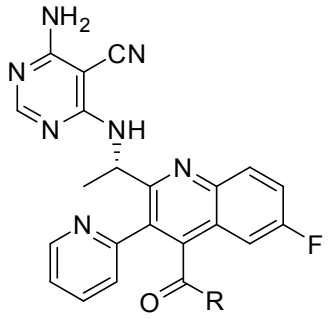

6a-e

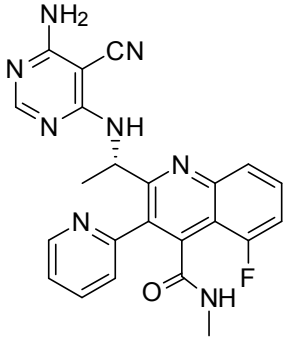

7

Cmpd	**R**	Biochemical potency[a]				Cellular potency		ADME Properties				Calculated properties
		PI3K IC_{50} (nM)				Human B cell[b]	Mouse B cell (pAKT)[c]	RLM / HLM[d]	CYP3A4 / 2D6[e]	hPXR[f]	Cl/ Clu[g]	clogP / LipE
		δ	α	β	γ	IC_{50} (nM)	IC_{50} (nM)	μL/(min.mg)	IC_{50} (μM)	POC @ 2 / 10 μM	L/hr/kg	
3	-	18	33000	2700	850	8.6	1.5	<14 / <14	>27 / >27	3 / 8	0.3/2.7	2.3 / 4.9
6a	–NHMe	2.9	17600	2840	3530	0.8	0.7	<14 / <14	>27 / >27	1 / 12	0.5/2.3	1.3 / 7.6
6b	–NHEt	3.6	16800	11000	5360	1.6	0.5	<14 / <14	>27 / >27	-1 / 5	0.2/6.1	1.8 / 6.9
6c[h]	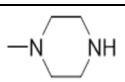	4.3	5750	7160	964	1.6	-	17 / 24	>27 / 27	0 / 7	-	1.2 / 7.4

6d[h]	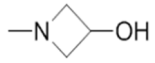	12	10900	4610	3590	7.4	-	<14 / <14	>27 / >27	1 / 4	-	1.2 / 7.1
6e	–NH(CH$_2$)$_2$NHMe	4.8	29200	15600	23200	1.2	8.5	<14 / 33	>27 / >27	2.4 / 4.9	1.0/28.1	1.7 / 6.6
7	-	4.6	14180	2200	3220	0.2	0.8	<14 / <14	>27 / >27	2 / 3	0.7/1.7	0.95 / 7.4

[a]Biochemical: Alphascreen assay; [b]Cellular: In vitro anti-IgM/CD40L-induced human B cell proliferation (as measured by thymidine incorporation) assay. [c]Cellular: Ability of compound to inhibit anti-IgM induced AKT phosphorylation (pAKT^{Ser473}) in mouse B cells; phospho-AKT (pAKT) expression on B220+gated B cells was determined by flow cytometry in mouse splenocytes. [d]Single experimental values. %Turnover was measured by LC/MS after incubation of parent compound (1 μM) in liver microsome (0.25 mg/mL) in potassium phosphate (66.7 mM) buffered with NADPH (1 mM) at 37 °C for 30 min. [e]CYP: cytochrome P450 assay competitive (midazolam as probe substrate, 5 μM) reported as % inhibition at 3 μM (LC/MS). [f]human Pregnane X Receptor. Data are shown as Percent of Control. [g]PK experiments were carried out using male Sprague-Dawley rats (n=3). Test compounds formulated at appropriate concentrations for IV (0.5 mL/kg). Unbound clearance equals the total clearance divided by the rat fraction unbound ($CL_u = CL/f_u$). [h]Racemic compound.

Table 2 illustrates the in vitro and in vivo data for the C3 pyridine analogs; consistent with our hypothesis, the PXR activation profile was significantly improved. The reduction in the clogP of these analogs did have an impact in their biochemical potency although the overall ligand efficiency was generally very good (lipE > 7 for most analogs). Among these PI3K inhibitors, the methyl amide substituted compound (**6a**, Table 2) displayed excellent levels of biochemical and cellular potency and similar PK profile relative to **3** (Clu = 2.3 vs Clu = 2.7). The potency profile of the ethyl amide analog **6b** was also very good although the Clu was about 3-fold higher that the parent inhibitor **6a**. The overall parameters of tertiary amides **6c** and **6d** were also satisfactory although the cellular potency of these analogs was reduced relative to **6a**. Having established the methyl amide in **6a** as the optimal substituent, the fluorination pattern of the quinoline ring was also explored. Contemporaneous work within the **3** series suggested that the C5 fluoro-quinoline substitution might be beneficial. Accordingly, **7** was prepared and had excellent potency and selectivity profile in biochemical and cellular assays as well as the best rat PK profile ever observed in this series (Clu = 1.7 L/hr/kg).

The potency and selectivity profiles of **3**, **6a** and **7** in biochemical, cellular and human whole blood assays are shown in Table 3. This data highlights the improved potency and isoform selectivity of **6a** and **7** relative to **3** in both biochemical and cellular assays. In the case of **6a**, the selectivity ratios over other isoforms were found to be improved relative to **3**. The intrinsic human whole blood assay data for **6a** and **7** was also determined and it

was found to be within 2.7 and 4.5-fold relative to **3** respectively, which was deemed suitable for further progression into in vivo studies.

Table 3: Profile of selected analogs.

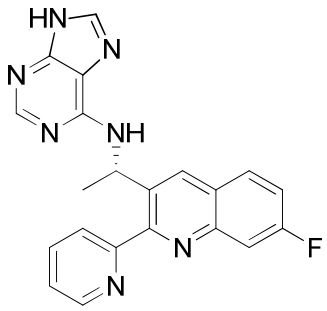

3

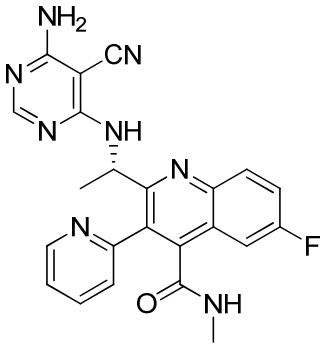

6a

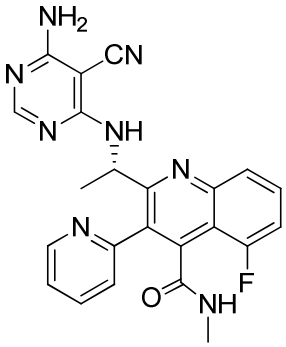

7

	PI3K Biochemical potency[a] IC$_{50}$ (nM) and PI3Kδ selectivity				PI3Kδ Cellular potency IC$_{50}$ (nM)			
Cmpd	δ	α/δ	β/δ	γ/δ	Human B cell[b]	Mouse B cell (pAKT)[c]	HWB (pAKT)[d]	HWB_unbound (pAKT)[e]
	(nM)	(ratio)	(ratio)	(ratio)	IC$_{50}$ (nM)	IC$_{50}$ (nM)	IC$_{50}$ (nM)	IC$_{50}$ (nM)
3	18	1833	150	47	8.6	1.5	10.9±2.5	1.7
6a	2.9	6068	979	1217	0.8	0.7	42±34	4.6
7	4.6	3082	478	700	0.2	0.8	18.5±11.5	7.7

[a]Biochemical: Alphascreen assay. [b]Cellular: In vitro anti-IgM/CD40L-induced human B cell proliferation (as measured by thymidine incorporation) assay. [c]Cellular: Ability of compound to inhibit anti-IgM induced AKT phosphorylation (pAKT^{Ser473}) in mouse B cells; phospho-AKT (pAKT) expression on B220+gate. [d] B cells was determined by flow cytometry in mouse splenocytes; compound pretreated human whole blood (HWB) was stimulated with anti-IgD to induce phosphorylation of AKT (pAKT^{Ser473}). [e]The unbound human whole blood (HWB_unbound) potency was derived by multiplying the human plasma protein binding (PPB) fraction unbound by the total HWB potency (f_u × HWB). [f]Cellular: Compound pretreated human whole blood (HWB) was stimulated with anti-IgD to induce CD-69 expression on B cells (6 hours) and was evaluated by flow cytometry.

The physicochemical properties and oral PK of these analogs is shown in Table 4. The solubility of both **6a** and **7** in PBS was comparable to that of **3** and these compounds also exhibited good passive permeability. The oral bioavailability of **6a** in the rat was found to be superior to both **3** and **7**, while the Clu remained low for all three analogs.

Table 4: Physicochemical properties and PK profile of selected analogs.

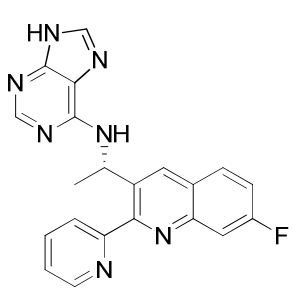

3

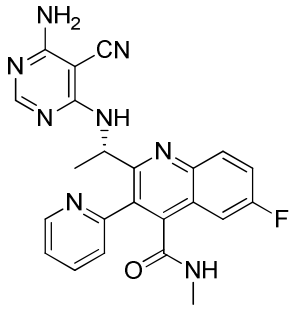

6a

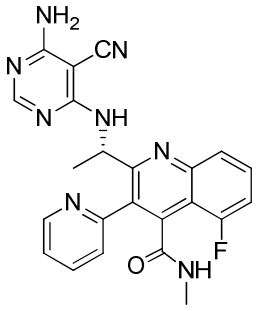

7

Cmpd	Solubility[a]	Permeability[b]	Protein Binding (f_u)		IV[e]		PO
	μg/mL	Papp x 10^{-6} cm/s	human[c]	rat[d]	Cl (L/h/Kg)	Cl_u (L/h/Kg)[f]	%F
3	>200	30	0.16	0.12	0.34	2.8	54
6a	200	14.6	0.11	0.22	0.51	2.3	70[g]
7	200	8	0.42	0.18	0.72	4.0	29[h]

[a]Single experimental values. Aqueous equilibrium solubility assay: compound was equilibrated at room temperature for 72 hours in PBS buffer (pH 7.4), supernatant was centrifuged and analyzed by HPLC for reporting solubility as μg/mL. [b]Passive permeability in LLCPK1 cells, apparent permeability (Papp) measured by mass balance (LC/MS). [c]5 μM concentration in human plasma, protein binding measured by ultracentrifugation and LC/MS. [d]5 μM concentration in rat plasma, protein binding measured by ultracentrifugation and LC/MS. [e]Pharmacokinetic parameters following administration in male Sprague-Dawley rats: two animals per study, dosed at 0.5 mg/kg as a solution in 100% DMSO. [f]Unbound clearance equals the total clearance divided by the rat fraction unbound ($CL_u = CL/f_u$). [g]Dosed at 2.0 mg/kg in 0.5% Tween 80, 1% methylcellulose, 98.5% water. [h]Dosed at 2.0 mg/kg in 0.5% methylcellulose, 1% Tween 80, 98.5% water.

Kinase selectivity profile and crystallography

Consistent with the profile of the **3** series, both quinolines, **6a** and **7**, were found to retain excellent kinase selectivity (KINOME*scan*'s selectivity score: S-Score(35)=0.013 for **6a**, S-Score(35)=0.008 for **7**) in a large panel of 442 protein kinases tested at 10 μM drug concentration.[24] This selectivity can be attributed to a common propeller-shaped conformation displayed by these molecules, illustrated by the X-ray co-crystal structure of analog **5g** with PI3Kγ (Figure 4). The improved biochemical potency of these analogs can also be rationalized by this co-crystal structure; the C4 substituent of the inhibitor makes additional interactions with the face of the Trp residue adjacent to the quinoline moiety (Trp812 in PI3Kγ, Trp760 in PI3Kδ).[25] Added flexibility in the position of this Trp residue in PI3Kδ relative to the other class I isoforms likely allows for

optimization of these additional interactions, thereby enhancing selectivity primarily through a greater potency boost to PI3Kδ compared to the other isoforms.

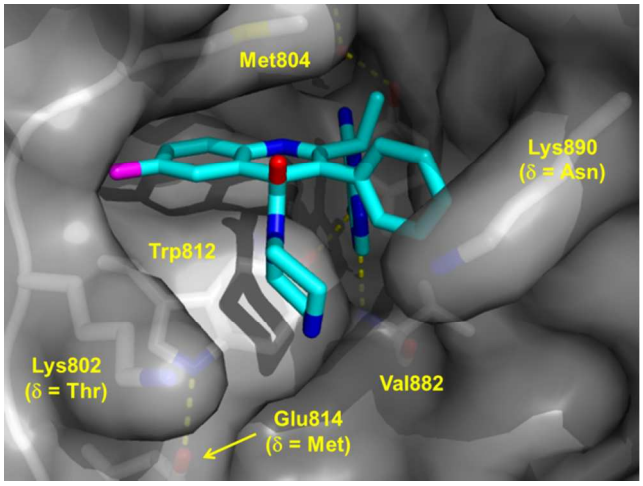

Figure 4. Crystal structure of PI3Kg in complex with compound **5g** (PDB code: 5KAE). Residues that differ in PI3Kd are labeled. Dashed lines indicate hydrogen bonds.

In Vivo Pharmacology

Given the improved selectivity of **6a** and **7** these analogs were advanced for evaluation in our in vivo animal models of inflammation. The in vivo experiments were performed with analogs **6a** and **7**, which were orally dosed to IgM_m mice[26] 15 minutes before an intravenous (IV) injection of FITC-labeled anti-IgM to stimulate circulation of B cells. The mice were sacrificed 30 minutes after stimulation to measure pAKT levels in spleen and whole blood of FITC-IgM positive B cells by flow cytometry (Figure 5). Both analogs **6a** and **7** showed dose-dependent inhibition of AKT phosphorylation in anti-IgM stimulated B cells isolated from the whole blood and spleen compartments of IgM_m mice. The calculated ED_{50} values for **6a** in spleen and whole blood were <0.01 mg/kg and <0.04 mg/kg, respectively (Figures 5a and 5b). The calculated ED_{50} values for **7** in splenocytes and whole blood were <0.003 mg/kg and 0.005 mg/kg, respectively (Figures 5c and 5d).

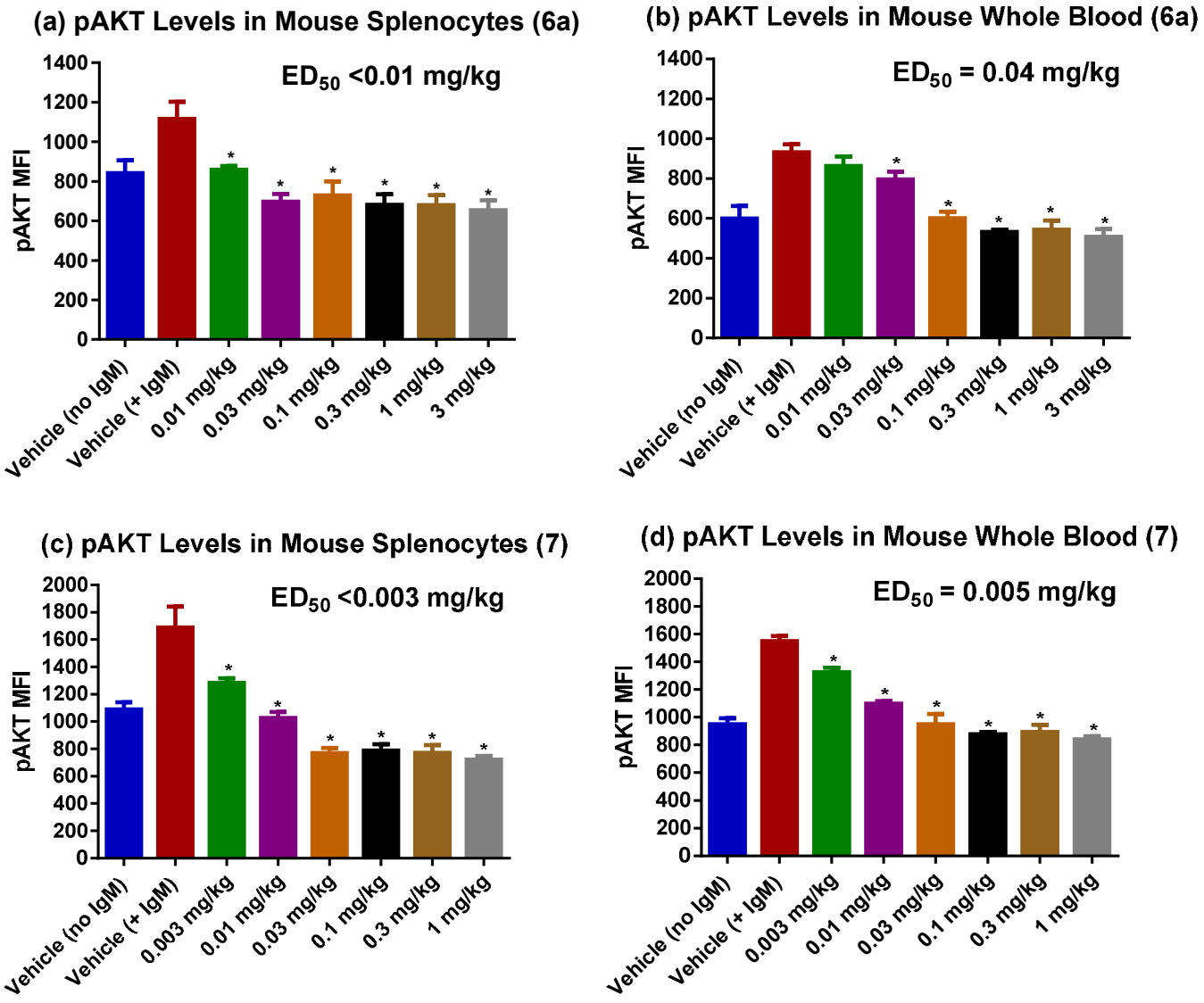

Figure 5. Inhibition of activation induced AKT phosphorylation in B cells in vivo. Vehicle, **6a**, **7** in 2% HPMC + 1% Tween 80, pH 2.0, was administered to IgM_m mice orally 15 minutes before intravenous (IV) injection of FITC-labeled anti-IgM to stimulate B cells. Mice were sacrificed 30 minutes after stimulation to measure pAKT in the spleen and whole blood of FITC-IgM positive B cells by flow cytometry. (a) pAKT of **6a** in splenocytes. (b) pAKT of **6a** in whole blood. (c) pAKT of **7** in splenocytes. (d) pAKT of **7** in whole blood-Test was used to evaluate differences between groups. The asterisk (*) denotes statistical significance ($p < 0.05$) when compared to the control group.

In a second in vivo experiment, the data from the in vivo pAKT assay was utilized to select doses for multi-dose rat protein-antigen (Keyhole Limpet Hemocyanin, KLH) studies. A multiple dose rat study was performed to determine whether **6a** and **7** could impact B cell function in vivo. For this purpose, the effect of **6a** and **7** on a humoral immune response, which is a measure of whether a compound inhibits antigen-specific Ig secretion by B cells, was studied via oral administration at multiple doses (Figures 6 and 7). These experiments

demonstrated that analog **6a** inhibited KLH-specific IgG and IgM in a dose-dependent manner (Figure 6a and Figure 6b). The calculated ED_{50} values were 0.026 mg/kg and 0.016 mg/kg, respectively. Exposure at these doses were expected to significantly inhibit PI3Kδ given the free drug concentrations achieved relative to the in vitro-derived pAKT_unbound IC_{50} (0.61 nM) over the 24 hours dosing interval (Figure 6c). Analog **7** inhibited KLH-specific IgG and IgM in a dose-dependent manner (Figure 7a and Figure 7b). The calculated ED_{50} values were 0.016 mg/kg and 0.015 mg/kg, respectively. Exposure at these doses were expected to significantly inhibit PI3Kδ given the free drug concentrations achieved relative to in vitro-derived pAKT_unbound IC_{50} (0.67 nM) over the 24 hours dosing interval (Figure 7c).

Exposure at all doses of **6a** and **7** were below in vitro PI3Kβ pAKT_unbound IC_{50} (2882 nM and 3500 nM, respectively) over 24 hours dosing interval (Figure 6c and Figure 7c). Additionally, both compounds, **6a** and **7**, were well tolerated at all doses. Ultimately, the KLH-mediated humoral immune response allowed us to select **6a** and **7** as candidates for further development.

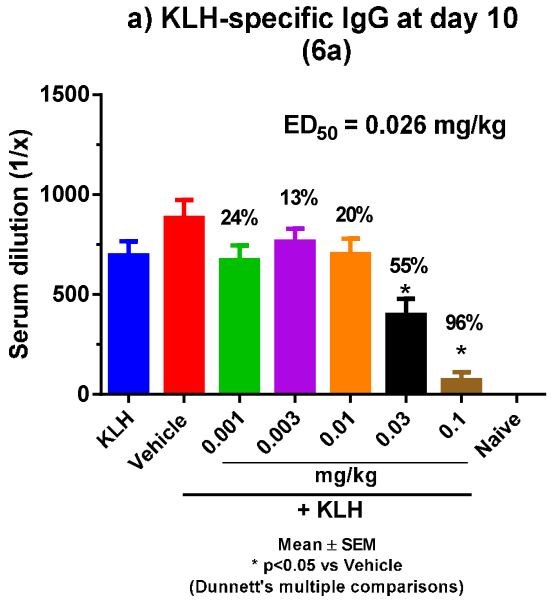

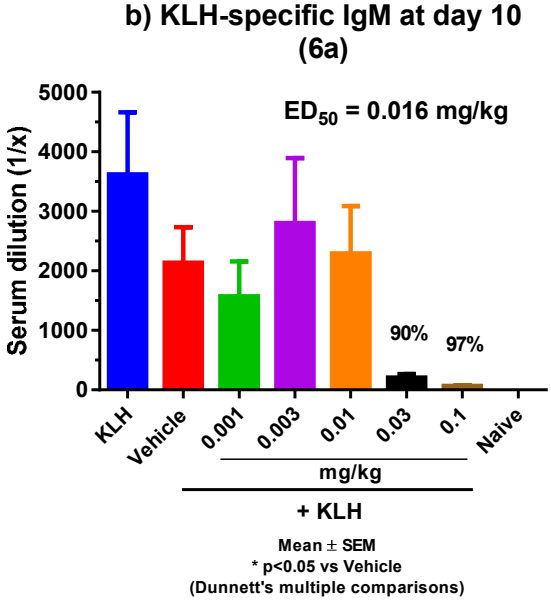

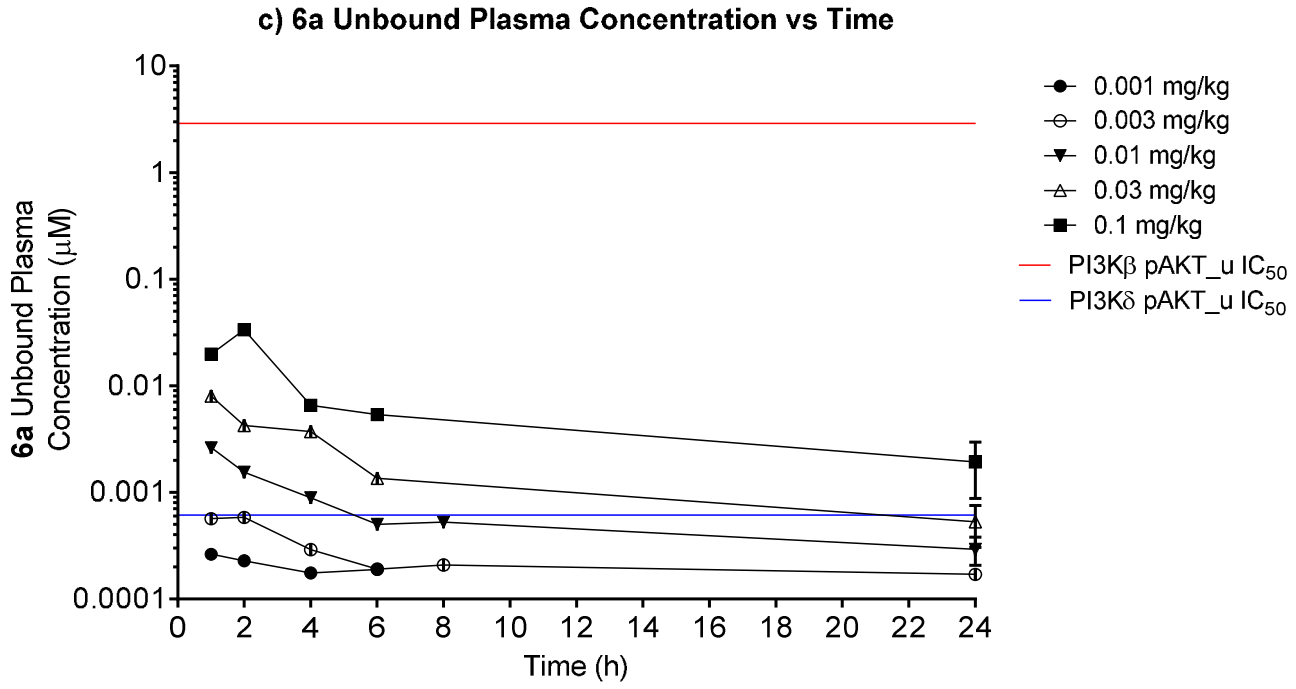

Figure 6. Inhibition of KLH-specific antibodies and delta-specific coverage. Vehicle or **6a** in 1% Pluronic F68, 2% HPMC, 10% Captisol, 87% water, was administered (0.001, 0.003, 0.01, 0.03, and 0.1 mg/kg) q.d. po for 10 days in female Lewis rats (N = 8/dose group). 2 hours after the first dosing, 200 μL of PBS containing 60 μg of KLH was administered to each rat intravenously. Ten days after the KLH priming, blood was collected for the measurement of KLH specific IgG (a) and IgM (b) by ELISA. The y-axis is represented as a mean serum dilution factor. Error bars represent the standard error of the mean (SEM) of eight rats. (c) After administration of **6a**, plasma was also harvested at day 10 to assess exposures in each dose group. Unbound drug concentrations were measured by LC−MS/MS and plotted relative to: PI3Kδ in vitro mouse pAKT_unbound IC_{50} 0.61 nM [calculated from 0.7 nM (PI3Kδ in vitro mouse pAKT IC_{50}) × 0.876 (f_u in pAKT assay media)] represented as a blue solid line; PI3Kβ in vitro human pAKT_unbound IC_{50} 2882 nM [calculated from 3290 nM (PI3Kβ in vitro human pAKT IC_{50}) × 0.876 (f_u in pAKT assay media)] represented as a red line.

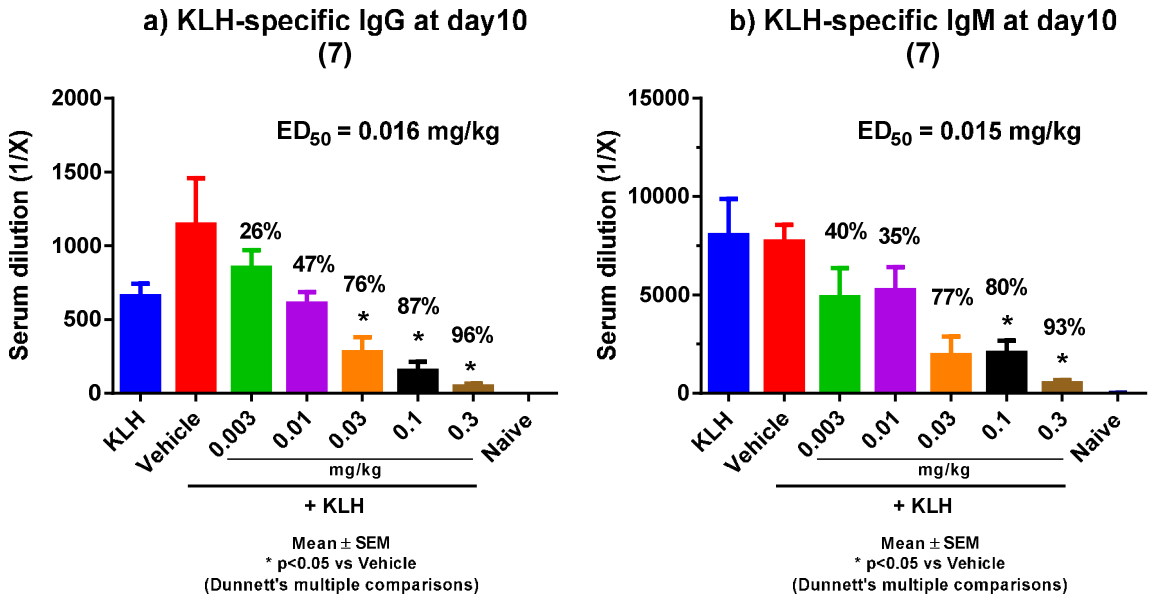

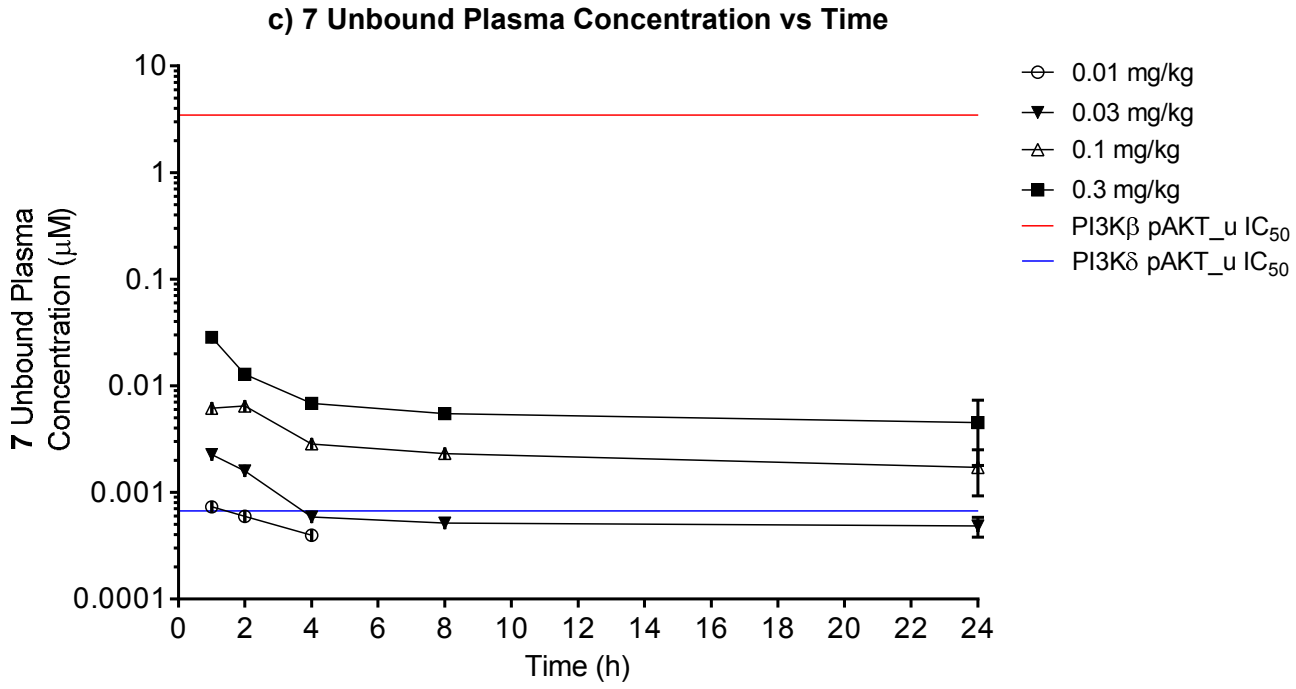

Figure 7. Inhibition of KLH-specific antibodies and delta-specific coverage. Vehicle or **7** in 1% Pluronic F68, 2% HPMC, 10% Captisol, 87% water, was administered (0.003, 0.01, 0.03, 0.1, and 0.3 mg/kg) q.d. po for 10 days in female Lewis rats (N = 8/dose group). 2 hours after the first dosing, 200 μL of PBS containing 60 μg of KLH was administered to each rat intravenously. Ten days after the KLH priming, blood was collected for the measurement of KLH specific IgG (a) and IgM (b) by ELISA. The y-axis is represented as a mean serum dilution factor. Error bars represent the standard error of the mean (SEM) of eight rats. (c) After administration of **7**, plasma was also harvested at day 10 to assess exposures in each dose group. Unbound drug concentrations were measured by LC−MS/MS and plotted relative to: PI3Kδ in vitro mouse pAKT_unbound IC_{50} 0.67 nM [calculated from 0.8 nM (PI3Kδ in vitro mouse pAKT IC_{50}) × 0.842 (f_u in pAKT assay media)] represented as a blue solid line; PI3Kβ in vitro human pAKT_unbound IC_{50} 3500 nM [calculated from 4110 nM (PI3Kβ in vitro human pAKT IC_{50}) × 0.842 (f_u in pAKT assay media)] represented as a red line.

CONCLUSION

A novel series of potent, selective and metabolically stable PI3Kδ inhibitors have been identified by optimizing the properties of the trisubstituted quinoline **4** (Figure 8). The successful strategy to improve the profile of this inhibitor involved modification of the pyridine ring at C4 and initial optimization within the C3 phenyl quinoline scaffold leading to the identification of a new series of amide analogs (e.g. **5b**). These new compounds had improved microsomal stability and isoform selectivity but unfavorable PXR activation profile. The latter issue was addressed by reducing the clogP of these molecules, which was accomplished by replacing the phenyl group at C3 (Figure 8, compound **5b**) with a pyridine ring. This strategy resulted in the

identification of **6a**, which upon further modification of the halogenation pattern led to the discovery of **7**. Both of these analogs showed satisfactory activity in both mice pAKT and rat KLH efficacy studies, which in combination with their optimal pharmacokinetic and selectivity profile, made them suitable candidates for further development.

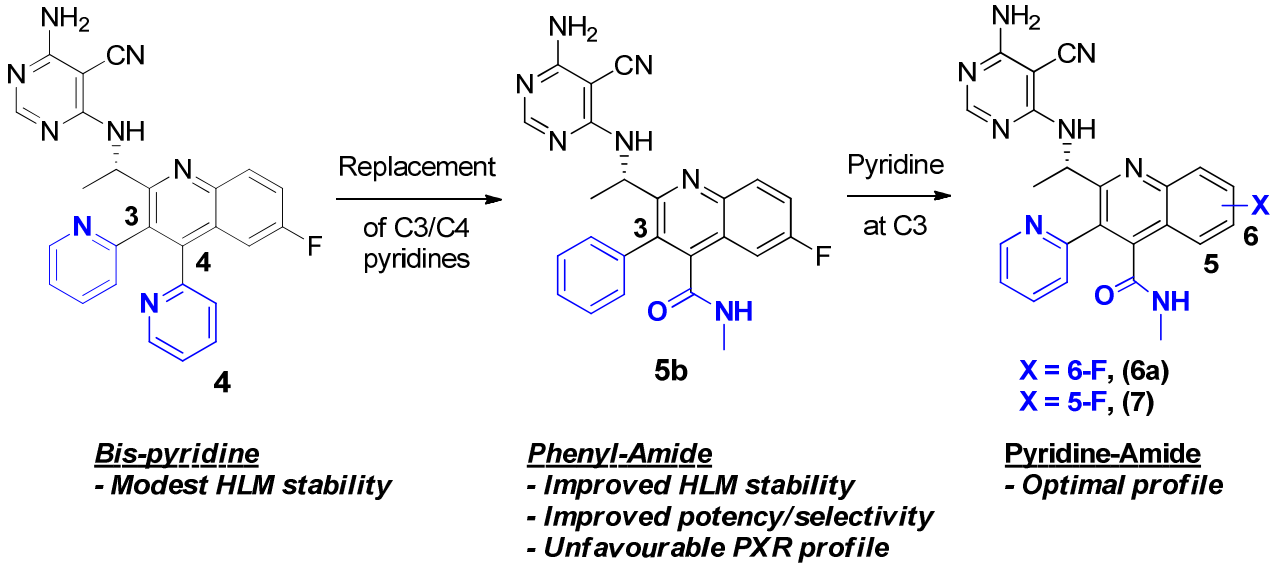

Figure 8. Evolution of the SAR leading to the identification of **6a** and **7**.

EXPERIMENTAL

All solvents and chemicals used were reagent grade. Anhydrous solvents were purchased from Sigma-Aldrich and used as received. Analytical thin layer chromatography (TLC) and silica gel column chromatography were performed on Merck silica gel 60 (230-400 mesh). Removal of solvents was conducted by using a rotary evaporator and residual solvents were removed from non-volatile compounds using a vacuum manifold maintained at approximately 1 Torr. All yields reported are isolated yields. Preparative reverse–phase high pressure liquid chromatography (RP–HPLC) was performed using an Agilent 1100 series HPLC and Phenomenex Gemini C18 column (5 μm, 100 mm × 30 mm i.d.), eluting with a binary solvent system, A and B, using a gradient elution [A, H_2O with 0.1% TFA, B, CH_3CN with 0.1% TFA] with UV detection at 220 nm.

All final compounds were purified to ≥95% purity as determined by an Agilent 1100 series HPLC with UV detection at 220 nm using the following method: Zorbax SB-C8 column (3.5 μm, 150 mm × 4.6 mm i.d.), eluting with a binary solvent system, A and B, using a 5-95% B (0-15 min) gradient elution [A, H_2O with 0.1% TFA, B, CH_3CN with 0.1% TFA]; flow rate 1.5 mL/min. Mass spectral data was recorded on an Agilent 1100 series LC-MS with UV detection at 254 nm. All accurate mass data (high-resolution mass spectra: HRMS) were acquired on a Synapt G2 Q-ToF instrument operating in positive electrospray ionization mode, over the *m/z* range 50-1200. Lock mass correction was performed on the leucine-enkephalin ion *m/z* 556.2771. The instrument resolution was 28,000 at FWHM. The compounds were introduced into the mass spectrometer using an Agilent 1200 operated with a C4 Bridged-ethyl-hybrid (BEH) analytical column (2.1 x 50 mm) at 0.25 mL/min. NMR spectra were recorded on a Bruker Avance 400 MHz and 500 MHz NMR spectrometer. Chemical shifts (δ) are reported in parts per million (ppm) relative to residual undeuterated solvent as internal reference and coupling constants (*J*) are reported in hertz (Hz). Splitting patterns are indicated as follows: s = singlet; d = doublet; t = triplet; q = quartet; qn = quintet; dd = doublet of doublets; dt = doublet of triplets; tt = triplet of triplets; m = multiplet; br = broad peak.

Preparative SFC method for chiral separation. Sample was dissolved in DCM-MeOH (2:1, 35 mg/mL). Column: AD-H (250 × 21 mm, 5 μm), AS-H (250 × 30 mm, 5 μm), IA-H (250 × 21 mm, 5 μm), Lux column (250 × 30 mm, 5 mm). Mobile Phase: A=Liquid CO_2; B=MeOH, EtOH, or isopropanol, Flow Rate: 70 mL/min. Column/Oven temperature: 40 ^oC. UV detection wavelength 220 nm. 20.7 mg/injection. 200 - 206 bar inlet pressure.

2-Ethyl-6-fluoro-3-phenylquinoline-4-carboxylic acid (9). A mixture of 5-fluoroisatin **8** (5.00 g, 30.3 mmol), 1-phenylbutan-2-one (4.99 mL, 33.3 mmol) and potassium hydroxide (5.10 g, 91 mmol) in EtOH (100 mL) was heated to reflux for 3 h. After cooling to r.t., the reaction mixture was concentrated in vacuo. The residue was

diluted with water and acidified with 1 N HCl to pH 5. The resulting solid was collected by filtration, washed with water, and dried to give 2-ethyl-6-fluoro-3-phenylquinoline-4-carboxylic acid **9** (8.60 g, 29.1 mmol, 96 % yield) as a fine tan powder. Mass spectrum (ESI) *m/z* 296.2 $[M+H]^+$.

Methyl 2-ethyl-6-fluoro-3-phenylquinoline-4-carboxylate (10). To a solution of 2-ethyl-6-fluoro-3-phenylquinoline-4-carboxylic acid **9** (8.60 g, 29.1 mmol) in DCM (100 mL) was added thionyl chloride (11.1 mL, 151 mmol) and the resulting mixture was stirred at r.t. overnight. The solvent was removed and MeOH (50 mL) was added and the resulting solution was stirred at r.t. for 2 h. The solvent was removed and crude residue was purified by column chromatography on silica gel using a 0-40% gradient of EtOAc/hexane as eluent to give methyl 2-ethyl-6-fluoro-3-phenylquinoline-4-carboxylate **10** (2.00 g, 6.47 mmol, 21% yield) as an off-white solid. ^{1}H-NMR (400 Hz, $CDCl_3$) δ 8.14 (dd, *J*=8.0, 4.0 Hz, 1H), 7.40-7.54 (m, 5H), 7.26-7.35 (m, 2H), 3.62 (s, 3H), 2.85 (q, *J*=8.0 Hz, 2H), 1.23 (t, *J*=8.0 Hz, 3H). Mass Spectrum (ESI) *m/z* 310 $[M+H]^+$.

Methyl 2-(1-bromoethyl)-6-fluoro-3-phenylquinoline-4-carboxylate (11). Methyl 2-ethyl-6-fluoro-3-phenylquinoline-4-carboxylate **10** (1.00 g, 3.2 mmol) and 1,3-dibromo-5,5-dimethylhydantoin (647 mg, 2.26 mmol) were suspended in carbon tetrachloride (30 mL) and treated with benzoyl peroxide (78 mg, 0.32 mmol) and the mixture was heated at reflux for 3 h. The reaction mixture was cooled to r.t. and treated with a saturated aqueous sodium bicarbonate solution. The layers were separated and the aqueous layer was extracted with DCM twice. The combined organic layers were washed with brine, dried over sodium sulfate, filtered, and concentrated in vacuo to give methyl 2-(1-bromoethyl)-6-fluoro-3-phenylquinoline-4-carboxylate **11** (1.40 g, 3.60 mmol, 56% yield) as a yellow solid. Mass Spectrum (ESI) *m/z* 388.0 $[M+H\ (^{79}Br)]^+$ and 390.0 $[M+H\ (^{81}Br)]^+$.

Methyl 2-(1-aminoethyl)-6-fluoro-3-phenylquinoline-4-carboxylate (12). To a solution of methyl 2-(1-bromoethyl)-6-fluoro-3-phenylquinoline-4-carboxylate **11** (1.17 g, 3.0 mmol) in DMF (6 mL) was added NaN_3

(0.293 g, 4.5 mmol) at r.t. After 2 h, the reaction mixture was diluted with water and extracted twice with EtOAc. The organic layers were combined, washed with water, brine, dried over Na_2SO_4, filtered, and concentrated in vacuo to give methyl 2-(1-azidoethyl)-6-fluoro-3-phenylquinoline-4-carboxylate as a tan oil. Mass Spectrum (ESI) *m/z* 351 $[M+H]^+$.

A solution of methyl 2-(1-azidoethyl)-6-fluoro-3-phenylquinoline-4-carboxylate (3.0 mmol) in MeOH (10 mL) was treated with 10% Pd/C (100 mg) and the mixture was stirred under an atmosphere of hydrogen gas at r.t. overnight. The reaction mixture was filtered through a Celite™ pad and concentrated in vacuo to give methyl 2-(1-aminoethyl)-6-fluoro-3-phenylquinoline-4-carboxylate **12** (0.92 g, 2.85 mmol, 95% yield) as a yellow oil. Mass Spectrum (ESI) *m/z* 325.2 $[M+H]^+$.

Methyl 2-(1-(6-amino-5-cyanopyrimidin-4-ylamino)ethyl)-6-fluoro-3-phenylquinoline-4-carboxylate (13). To the solution of methyl 2-(1-aminoethyl)-6-fluoro-3-phenylquinoline-4-carboxylate **12** (660 mg, 2.04 mmol) in *n*-BuOH (6 mL) was added 4-amino-6-chloropyrimidine-5-carbonitrile (314 mg, 2.04 mmol) and DIPEA (0.43 mL, 2.44 mmol) and the resulting mixture was heated to 120 °C for 3 h. The reaction mixture was cooled to r.t., diluted with water, and extracted with EtOAc (2 × 20 mL). The organic layers were combined, washed with water, brine, dried over Na_2SO_4, filtered, concentrated and purified by column chromatography on silica gel (DCM/MeOH/NH_3, 20/1/0.1) to give methyl 2-(1-(6-amino-5-cyanopyrimidin-4-ylamino)ethyl)-6-fluoro-3-phenylquinoline-4-carboxylate (747 mg, 1.69 mmol, 83% yield) as an off-white solid. ^{1}H-NMR (400 Hz, DMSO-d_6) δ 8.16 (dd, *J*=8.0, 4.0 Hz, 1H), 7.91 (s, 1H), 7.81 (td, *J*=8.0, 4.0 Hz, 1H), 7.59 (dd, *J*=8.0, 4.0 Hz, 1H), 7.45-7.52 (m, 5H), 7.35 (dd, *J*=8.0, 4.0 Hz, 1H), 7.25 (s, br, 2H), 5.30-5.40 (m, 1H), 3.59 (s, 3H), 1.30 (t, *J*=8.0 Hz, 3H). Mass Spectrum (ESI) *m/z* 443.2 $[M+H]^+$.

2-(1-(6-Amino-5-cyanopyrimidin-4-ylamino)ethyl)-6-fluoro-3-phenylquinoline-4-carboxylic acid (14). To a suspension of methyl 2-(1-(6-amino-5-cyanopyrimidin-4-ylamino)ethyl)-6-fluoro-3-phenylquinoline-4-

carboxylate **13** (1.09 g, 2.47 mmol) in pyridine (20 mL) was added lithium iodide (0.99 g, 7.40 mmol) and the resulting mixture was stirred at 100 °C overnight. The mixture was concentrated in vacuo. The residue was suspended in water and the aqueous mixture was acidified with 1 N HCl to pH 5. The resulting solid was collected by filtration, washed with water, and dried to give 2-(1-(6-amino-5-cyanopyrimidin-4-ylamino)ethyl)-6-fluoro-3-phenylquinoline-4-carboxylic acid (1.04 g, 2.43 mmol, 98% yield) as a white solid. ^{1}H-NMR (400 Hz, DMSO-d_6) δ 8.16 (dd, *J*=8.0, 4.0 Hz, 1H), 7.97 (s, 1H), 7.81 (td, *J*=8.0, 4.0 Hz, 1H), 7.72 (dd, *J*=8.0, 4.0 Hz, 1H), 7.38-7.52 (m, 8H), 5.30-5.40 (m, 1H), 1.30 (t, *J*=8.0 Hz, 3H). Mass Spectrum (ESI) *m/z* 429.2 $[M+H]^+$.

(*S*)-2-(1-(6-Amino-5-cyanopyrimidin-4-ylamino)ethyl)-6-fluoro-3-phenylquinoline-4-carboxylic acid (15). The racemic mixture **14** was purified with an AD-H column using 22% isopropanol (0.2% diethylamine) as additive B in supercritical CO_2. Compound **15** was the first eluting enantiomer and isolated as a yellow solid (45% yield). Mass spectrum (ESI) *m/z* 429.2 $[M+H]^+$.

General Procedure for the Synthesis of 5a-c and f-i. To a solution of (*S*)-2-(1-(6-amino-5-cyanopyrimidin-4-ylamino)ethyl)-6-fluoro-3-phenylquinoline-4-carboxylic acid **15** (0.16 mmol) in DMF (1 mL) was added amine (1.5 equiv.), DIPEA (1.1 equiv.), and PyBop (2.2 equiv.) and the resulting mixture was stirred at r.t. for 1 h. The mixture was concentrated in vacuo. The residue was dissolved in EtOAc and washed with water, brine, dried over sodium sulfate, filtered, and concentrated in vacuo. The crude product was purified by column chromatography on silica gel using 0-100% EtOAc/hexane as eluent or preparative HPLC to give **5a-c, f-i**.

2-((1*S*)-1-((6-Amino-5-cyano-4-pyrimidinyl)amino)ethyl)-6-fluoro-3-phenyl-4-quinolinecarboxamide (5a). Obtained in 20% yield as a white solid. (400 MHz, CD_3OD) δ ppm 8.19 (1 H, dd, *J*=9.2, 5.3 Hz), 8.10 (1 H, s), 7.64 - 7.71 (1 H, m), 7.59 (1 H, dd, *J*=9.4, 2.7 Hz), 7.43 - 7.52 (5 H, m), 5.58 (1 H, q, *J*=6.7 Hz), 1.43 (3 H, d,

J=6.8 Hz). Mass spectrum (ESI) *m/z* 428.2 $[M+H]^+$. HRMS (ESI) *m/z* calculated for $C_{23}H_{18}FN_7O$ $[M+H]^+$: 428.1635; mass measured, 428.1629.

2-((1*S*)-1-((6-Amino-5-cyano-4-pyrimidinyl)amino)ethyl)-6-fluoro-*N*-methyl-3-phenyl-4-quinolinecarboxamide (5b). Obtained in 27% yield as a white solid. ^{1}H NMR (400 MHz, DMSO-d_6) δ ppm 8.34 - 8.43 (1 H, m), 8.13 (1 H, dd, *J*=9.2, 5.5 Hz), 7.95 (1 H, s), 7.78 (1 H, td, *J*=8.8, 2.7 Hz), 7.36 - 7.54 (7 H, m), 7.29 (2 H, br s), 5.35 (1 H, quin, *J*=6.7 Hz), 2.53 (3 H, d, *J*=4.7 Hz), 1.26 (3 H, d, *J*=6.7 Hz). Mass Spectrum (ESI) *m/z* 442.0 $[M+H]^+$. HRMS (ESI) *m/z* calculated for $C_{24}H_{20}FN_7O$ $[M+H]^+$: 442.1792; mass measured, 442.1784.

2-((1*S*)-1-((6-Amino-5-cyano-4-pyrimidinyl)amino)ethyl)-6-fluoro-*N*,*N*-dimethyl-3-phenyl-4-quinolinecarboxamide (5c). Obtained in 26% yield as a white solid. ^{1}H NMR (400 MHz, CD_3OD) δ ppm 8.21 (1 H, dd, *J*=9.2, 5.3 Hz), 7.98 (1 H, s), 7.64 - 7.71 (1 H, m), 7.57 - 7.62 (1 H, m), 7.48 - 7.56 (3 H, m), 7.40 - 7.47 (1 H, m), 7.36 (1 H, dd, *J*=9.3, 2.6 Hz), 5.61 (1 H, q, *J*=6.6 Hz), 2.84 (3 H, s), 2.60 (3 H, s), 1.26 (3 H, d, *J*=6.7 Hz). Mass Spectrum (ESI) *m/z* 456.2 $[M+H]^+$. HRMS (ESI) *m/z* calculated for $C_{25}H_{22}FN_7O$ $[M+H]^+$: 456.1948; mass measured, 456.1946.

4-Amino-6-(((1*S*)-1-(4-((1,1-dioxido-4-thiomorpholinyl)carbonyl)-6-fluoro-3-phenyl-2-quinolinyl)ethyl)amino)-5-pyrimidinecarbonitrile (5f). Obtained in 13% yield as a white solid. Mass Spectrum (ESI) *m/z* 546.2 $[M+H]^+$. HRMS (ESI) *m/z* calculated for $C_{27}H_{24}FN_7O_3S$ $[M+H]^+$: 546.1724; mass measured, 546.1807.

4-Amino-6-(((1*S*)-1-(6-fluoro-3-phenyl-4-(1-piperazinylcarbonyl)-2-quinolinyl)ethyl)amino)-5-pyrimidinecarbonitrile (5g). Obtained in 40% yield as a white solid. ^{1}H NMR (400 MHz, CD_3OD) δ ppm 8.22 - 8.27 (1 H, m), 8.21 (1 H, s), 7.72 (1 H, td, *J*=8.9, 2.8 Hz), 7.64 - 7.68 (1 H, m), 7.47 - 7.63 (6 H, m), 5.80 (1 H, q, *J*=6.8 Hz), 3.87 (1 H, ddd, *J*=14.5, 7.5, 3.4 Hz), 3.66 (1 H, ddd, *J*=14.5, 6.8, 3.5 Hz), 3.34 - 3.39 (1 H,

m), 3.22 - 3.29 (1 H, m), 3.10 - 3.20 (1 H, m), 2.89 - 3.01 (1 H, m), 2.63 - 2.75 (1 H, m), 2.45 - 2.54 (1 H, m), 1.28 (3 H, d, *J*=6.7 Hz). Mass Spectrum (ESI) *m/z* 497.0 $[M+H]^+$. HRMS (ESI) *m/z* calculated for $C_{27}H_{25}FN_8O$ $[M+H]^+$: 497.2214; mass measured, 497.2216.

4-Amino-6-(((1*S*)-1-(6-fluoro-4-((3-hydroxy-1-azetidinyl)carbonyl)-3-phenyl-2-quinolinyl)ethyl)amino)-5-pyrimidinecarbonitrile (5h). Obtained in 71% yield as a white solid. ^{1}H NMR (400 MHz, CD_3OD) δ ppm 8.17 - 8.25 (1 H, m), 8.00 (1 H, d, *J*=1.4 Hz), 7.85 (1 H, d, *J*=5.3 Hz), 7.39 - 7.73 (6 H, m), 5.42 - 5.70 (1 H, m), 4.01 - 4.65 (2 H, m), 3.40 - 3.99 (3 H, m), 1.20 - 1.58 (3 H, m). Mass Spectrum (ESI) *m/z* 484.2 $[M+H]^+$. HRMS (ESI) *m/z* calculated for $C_{26}H_{22}FN_7O_2$ $[M+H]^+$: 484.1897; mass measured, 484.1899.

2-((1*S*)-1-((6-Amino-5-cyano-4-pyrimidinyl)amino)ethyl)-6-fluoro-*N*-(2-(methylamino)ethyl)-3-phenyl-4-quinolinecarboxamide (5i). Obtained in 99% yield as a white solid. ^{1}H NMR (400 MHz, CD_3OD) δ ppm 8.21 (1 H, dd, *J*=9.3, 5.4 Hz), 8.12 (1 H, s), 7.68 (1 H, ddd, *J*=9.3, 8.4, 2.8 Hz), 7.41 - 7.58 (6 H, m), 5.62 (1 H, q, *J*=6.7 Hz), 3.35 - 3.48 (2 H, m), 2.64 - 2.69 (2 H, m), 2.62 (3 H, s), 1.45 (3 H, d, *J*=6.7 Hz). Mass Spectrum (ESI) *m/z* 485.2 $[M+H]^+$. HRMS (ESI) *m/z* calculated for $C_{26}H_{25}FN_8O$ $[M+H]^+$: 485.2214; mass measured, 485.2213.

(*S*)-Methyl 2-(1-(*tert*-butoxycarbonylamino)ethyl)-6-fluoro-3-phenylquinoline-4-carboxylate (16). To a solution of methyl 2-(1-aminoethyl)-6-fluoro-3-phenylquinoline-4-carboxylate **12** (2.45 g, 7.55 mmol) in THF (30 mL) was added Boc-anhydride (1.65 g, 7.55 mmol) followed by triethylamine (1.05 mL, 7.55 mmol) and the reaction mixture was stirred at r.t. After 30 min, the solvent was concentrated in vacuo and the crude product was purified by column chromatography on silica gel using 0-30% EtOAc/hexane to afford methyl 2-(1-(*tert*-butoxycarbonylamino)ethyl)-6-fluoro-3-phenylquinoline-4-carboxylate (2.47 g, 5.82 mmol, 77% yield) as a white powder. Mass Spectrum (ESI) *m/z* 425.2 $[M+H]^+$.

The racemic mixture was purified with AS-H column using 5% methanol in supercritical CO_2. Compound **16** was the second eluting enantiomer and isolated as a yellow solid (44% yield). Mass spectrum (ESI) *m/z* 425.2 $[M+H]^+$.

General Procedure for the Synthesis of 17d,e. To a solution of (*S*)-methyl 2-(1-(*tert*-butoxycarbonylamino)ethyl)-6-fluoro-3-phenylquinoline-4-carboxylate **16** (4.43 g, 10.4 mmol) in MeOH (50 mL) was added NaOH (50 mL, 10.4 mmol) and the resulting mixture was stirred at 60 °C overnight. The reaction mixture was allowed to cool to r.t. and MeOH was removed. The mixture was acidified with 2N HCl to pH 2. The resulting precipitate was collected by filtration and dried to obtain (*S*)-2-(1-(*tert*-butoxycarbonylamino)ethyl)-6-fluoro-3-phenylquinoline-4-carboxylic acid (4.30 g, 10.48 mmol, 99% yield) as a light yellow powder.

To a solution of (*S*)-2-(1-(*tert*-butoxycarbonylamino)ethyl)-6-fluoro-3-phenylquinoline-4-carboxylic acid (0.16 mmol) in DMF (1 mL) was added amine (2 equiv.), DIPEA (3 equiv.), and PyBop (2.5 equiv.) and the resulting mixture was stirred at r.t. overnight. The crude mixture was purified by column chromatography on silica gel using 0-100% EtOAc/hexane as eluent to give **17d,e**.

(*S*)-*tert*-Butyl 1-(4-(ethylcarbamoyl)-6-fluoro-3-phenylquinolin-2-yl)ethylcarbamate (17d). Obtained in 69% yield. Mass Spectrum (ESI) *m/z* 438.2 $[M+H]^+$.

(*S*)-*tert*-Butyl 1-(6-fluoro-4-(isopropylcarbamoyl)-3-phenylquinolin-2-yl)ethylcarbamate (17e). Obtained in 86% yield. Mass Spectrum (ESI) *m/z* 452.2 $[M+H]^+$.

General Procedure for the Synthesis of 5d,e. To a crude residue of **17d** or **17e** (0.051 mmol) was added HCl (0.5 mL, 2.000 mmol) and the resulting mixture was stirred at r.t. for 1 h. The mixture was concentrated in vacuo and the crude product was carried on crude for next step.

To a solution of *(S)*-2-(1-aminoethyl)-N-ethyl-6-fluoro-3-phenylquinoline-4-carboxamide or *(S)*-2-(1-aminoethyl)-6-fluoro-N-isopropyl-3-phenylquinoline-4-carboxamide in *n*-BuOH (0.5 mL) was added DIEA (0.026 mL, 0.152 mmol) and 4-amino-6-chloropyrimidine-5-carbonitrile (7.81 mg, 0.051 mmol) . The resulting mixture was stirred and heated at 100 °C overnight. The reaction mixture was cooled to r.t., diluted with water, and extracted with EtOAc (2 × 20 mL). The organic layers were combined, washed with water, brine, dried over Na_2SO_4, filtered, concentrated and purified by column chromatography on silica gel (DCM/MeOH/NH_3, 20/1/0.1) to give **5d,e**.

2-((1*S*)-1-((6-Amino-5-cyano-4-pyrimidinyl)amino)ethyl)-*N*-ethyl-6-fluoro-3-phenyl-4-quinolinecarboxamide (5d). Obtained in 31% yield as a white solid. ^{1}H NMR (400 MHz, CD_3OD) δ ppm 8.47 (1 H, br t, *J*=5.4 Hz), 8.19 (1 H, dd, *J*=9.2, 5.3 Hz), 8.10 (1 H, s), 7.63 - 7.71 (1 H, m), 7.40 - 7.54 (6 H, m), 5.60 (1 H, q, *J*=6.8 Hz), 3.11 - 3.22 (2 H, m), 1.44 (3 H, d, *J*=6.7 Hz), 0.79 (3 H, t, *J*=7.2 Hz). Mass Spectrum (ESI) *m/z* 456.2 $[M+H]^+$. HRMS (ESI) *m/z* calculated for $C_{25}H_{22}FN_7O$ $[M+H]^+$: 456.1948; mass measured, 456.1942.

2-((1*S*)-1-((6-amino-5-cyano-4-pyrimidinyl)amino)ethyl)-6-fluoro-*N*-(1-methylethyl)-3-phenyl-4-quinolinecarboxamide (5e). Obtained in 68% yield as a white solid. ^{1}H NMR (400 MHz, CD_3OD) δ ppm 8.19 (1 H, dd, *J*=9.2, 5.3 Hz), 7.92 - 7.97 (1 H, m), 7.65 (1 H, td, *J*=8.8, 2.7 Hz), 7.38 - 7.54 (6 H, m), 5.53 (1 H, q, *J*=6.5 Hz), 3.94 (1 H, dt, *J*=13.1, 6.6 Hz), 1.35 (3 H, d, *J*=6.7 Hz), 0.96 (3 H, br d, *J*=6.5 Hz), 0.81 (3 H, br d, *J*=6.5 Hz). Mass Spectrum (ESI) *m/z* 470.2 $[M+H]^+$. HRMS (ESI) *m/z* calculated for $C_{26}H_{24}FN_7O$ $[M+H]^+$: 470.2105; mass measured, 470.2107.

2-Ethyl-6-fluoro-3-(pyridin-2-yl)quinoline-4-carboxylic acid (18). A mixture of compound **8** (22.0 g, 133 mmol), 1-(pyridin-2-yl)butan-2-one (19.9 g, 133 mmol), KOH (22.5 g, 400 mmol), EtOH (100 mL) and water (100 mL) was stirred and heated at 90 °C overnight. After cooling to r.t., the reaction mixture was concentrated

in vacuo. The residue was diluted with water and acidified with 1 N HCl to pH 5. The resulting solid was collected by filtration, washed with water, and dried give 2-ethyl-6-fluoro-3-(pyridin-2-yl)quinoline-4-carboxylic acid **18** (39.0 g. 132 mmol, 99% yield) as an off-white solid.

Methyl 2-ethyl-6-fluoro-3-(pyridin-2-yl)quinoline-4-carboxylate (19). To a solution of **18** (15 g, 50.6 mmol) in MeOH (75 mL) at 0 °C was added $TMSCHN_2$ (2 M in DCM, 6.2 mL, 93 mmol) and the mixture was allowed to warm to r.t. After 2 h, the mixture was concentrated in vacuo and purified by column chromatography on silica gel using 30% EtOAc/hexane to give methyl 2-ethyl-6-fluoro-3-(pyridin-2-yl)quinoline-4-carboxylate **19** (4.60 g, 14.82 mmol, 29% yield) as a pink solid. ^{1}H NMR (400 MHz, CHLOROFORM-d) δ ppm 8.71 - 8.82 (1 H, m), 8.08 - 8.19 (1 H, m), 7.82 (1 H, td, *J*=7.7, 1.8 Hz), 7.49 - 7.60 (2 H, m), 7.43 (1 H, dt, *J*=7.8, 1.0 Hz), 7.36 (1 H, ddd, *J*=7.6, 4.9, 1.2 Hz), 3.65 (3 H, s), 2.92 (2 H, q, *J*=7.5 Hz), 1.23 (3 H, t, *J*=7.5 Hz).

Methyl 2-(1-bromoethyl)-6-fluoro-3-(pyridin-2-yl)quinoline-4-carboxylate (20). To a solution of **19** (0.300 g, 0.967 mmol) in carbon tetrachloride (9 mL) was added 1,3-dibromo-5,5-dimethylimidazolidine-2,4-dione (0.193 g, 0.677 mmol) followed by benzoyl peroxide (0.023 g, 0.097 mmol) and the mixture was heated to reflux overnight. The mixture was washed with a saturated sodium bicarbonate, brine, and dried over sodium sulfate and activated carbon. The mixture was filtered and concentrated in vacuo to give methyl 2-(1-bromoethyl)-6-fluoro-3-(pyridin-2-yl)quinoline-4-carboxylate **20** (302 mg, 0.776 mmol, 80% yield). Mass Spectrum (ESI) *m/z* 389.0 $[M+H\ (^{79}Br)]^+$ and 391.1 $[M+H\ (^{81}Br)]^+$.

Methyl 2-(1-aminoethyl)-6-fluoro-3-(pyridin-2-yl)quinoline-4-carboxylate (21). To a solution of **20** (2.94 g, 7.54 mmol) in DMF (15 mL) was added sodium azide (0.736 g, 11.31 mmol) and the mixture was stirred at r.t. After 1 h, the mixture was diluted with EtOAc, washed with water, brine, and dried over sodium sulfate. The mixture was filtered and the filtrate was concentrated in vacuo to afford methyl 2-(1-azidoethyl)-6-fluoro-3-(pyridin-2-yl)quinoline-4-carboxylate (2.85 g, 8.11 mmol, quantitative yield) as a green oil.

Methyl 2-(1-azidoethyl)-6-fluoro-3-(pyridin-2-yl)quinoline-4-carboxylate (2.85 g, 8.11 mmol) was dissolved in MeOH (20 mL). To the solution was added 10% Pd/C (0.129 g) and the resulting suspension was stirred under hydrogen at r.t. After 45 min, the reaction mixture was filtered through a Celite pad and the solvent was removed under reduced pressure to afford methyl 2-(1-aminoethyl)-6-fluoro-3-(pyridin-2-yl)quinoline-4-carboxylate **21** (2.26 g, 6.95 mmol, 86% yield) as a dark brown oil. Mass Spectrum (ESI) *m/z* 326.2 $[M+H]^+$.

Methyl 2-(1-(6-amino-5-cyanopyrimidin-4-ylamino)ethyl)-6-fluoro-3-(pyridin-2-yl)quinoline-4-carboxylate (22). To the solution of **21** (1.50, 4.61 mmol) in *n*-BuOH (4 mL) was added 4-amino-6-chloropyrimidine-5-carbonitrile (0.713 g, 4.61 mmol) and DIPEA (1.6 mL, 9.22 mmol) and the resulting mixture was heated to 100 °C overnight. The solvent was removed and the crude residue recrystallized with EtOAc/hexane to obtain methyl 2-(1-(6-amino-5-cyanopyrimidin-4-ylamino)ethyl)-6-fluoro-3-(pyridin-2-yl)quinoline-4-carboxylate **22** (2.00 g, 4.51 mmol, 98% yield). Mass Spectrum (ESI) *m/z* 444.2 $[M+H]^+$.

2-(1-(6-Amino-5-cyanopyrimidin-4-ylamino)ethyl)-6-fluoro-3-(pyridin-2-yl)quinoline-4-carboxylic acid (23). A suspension of **22** (2.00 g, 4.51 mmol) in pyridine (20 mL) was treated with lithium iodide (1.81 g, 13.53 mmol) and the resulting mixture was stirred at 100 °C overnight. The mixture was concentrated in vacuo and the crude residue was suspended in water and the aqueous mixture was acidified with 1N HCl to pH 5. The resulting solid was extracted twice with EtOAc and the combined organic extracts was washed with brine and dried over sodium sulfate, filtered, and concentrated in vacuo to give 2-(1-(6-amino-5-cyanopyrimidin-4-ylamino)ethyl)-6-fluoro-3-(pyridin-2-yl)quinoline-4-carboxylic acid **23** (1.90 g, 4.42 mmol, 98% yield) as a white solid. ^{1}H NMR (400 MHz, CD_3OD) δ ppm 8.74 (1 H, d, *J*=5.1 Hz), 8.21 - 8.28 (1 H, m), 8.03 - 8.11 (2 H, m), 7.68 - 7.78 (3 H, m), 7.59 (1 H, ddd, *J*=7.1, 5.8, 1.0 Hz), 5.62 (1 H, q, *J*=6.5 Hz), 1.46 (3 H, d, *J*=6.7 Hz). Mass Spectrum (ESI) *m/z* 430.2 $[M+H]^+$.

(*S*)-*tert*-Butyl 3-oxo-4-(pyridin-2-yl)butan-2-ylcarbamate (24). To a solution of picoline (31.9 mL, 323 mmol) in THF (300 mL) was added MeLi (1.6M in hexanes, 202 mL, 323 mmol) drop-wise at -40 °C under nitrogen. The reaction mixture was allowed to warm to -20 °C and stirred for 10 min and then cooled to -40 °C and magnesium bromide (59.4 g, 323 mmol) was added in three portions. The reaction mixture was allowed to warm to r.t., stirred for 30 min to provide bromo(pyridin-2-ylmethyl)magnesium (323 mmol).

tert-Butyl-1-(methoxy(methyl)amino)-1-oxopropan-2-ylcarbamate (50.0 g, 215 mmol) in THF (450 mL) was cooled to -40 °C (dry ice/acetonitrile) and slowly charged with isopropylmagnesium chloride (2.0M in Et_2O, 102 mL, 204 mmol). After a clear solution was obtained (became clear at -20 °C and milky again at -40 °C), bromo(pyridin-2-ylmethyl)magnesium solution (323 mmol) was added drop-wise using a cannula before warming to r.t. overnight. The reaction mixture was quenched with a saturated NH_4Cl solution and extracted with EtOAc twice. The combined organic layers were washed with water, brine, dried over sodium sulfate, filtered, and concentrated in vacuo. The crude product was purified by column chromatography on a silica gel column using 0-30% gradient of EtOAc/hexane as eluent to give (*S*)-*tert*-butyl 3-oxo-4-(pyridin-2-yl)butan-2-ylcarbamate **24** (40.0 g, 151 mmol, 70% yield) as a tan oil. Mass Spectrum (ESI) *m/z* 265.1 $[M+H]^+$.

2-(1-(*tert*-Butoxycarbonylamino)ethyl)-6-fluoro-3-(pyridin-2-yl)quinoline-4-carboxylic acid (25). A mixture of KOH (25.0 g, 446 mmol) and 5-fluoroisatin **8** (36.9 g, 223 mmol) in EtOH (100 mL) and water (350 mL) were stirred at r.t. for 30 min before addition of (*S*)-*tert*-butyl 3-oxo-4-phenylbutan-2-ylcarbamate **24** (59.00 g, 223 mmol). The reaction mixture was heated to 85 °C overnight and cooled to r.t. The reaction mixture was concentrated in vacuo to remove EtOH. The mixture was diluted with water and acidified with concentrated HCl to pH 2. The mixture was extracted twice with DCM. The combined organic extracts were dried over $MgSO_4$, filtered, and concentrated in vacuo to give 2-(1-(*tert*-butoxycarbonylamino)ethyl)-6-fluoro-3-(pyridin-2-yl)quinoline-4-carboxylic acid **25** (71.70 g, 174 mmol, 78% yield) as a pale yellow solid. ^{1}H NMR (500 MHz, DMSO-d_6) δ ppm 8.70 (1 H, br d, *J*=4.6 Hz), 8.19 (1 H, dd, *J*=9.2, 5.5 Hz), 7.96 (1 H, td, *J*=7.7, 1.5

Hz), 7.79 (1 H, td, *J*=8.8, 2.7 Hz), 7.51 - 7.63 (2 H, m), 7.47 (1 H, dd, *J*=7.2, 5.3 Hz), 7.08 (1 H, br d, *J*=7.6 Hz), 4.86 (1 H, br t, *J*=7.1 Hz), 1.30 (9 H, s), 1.22 (3 H, br d, *J*=6.8 Hz). Mass Spectrum (ESI) *m/z* 412.2 $[M+H]^+$.

General Procedure for the Synthesis of 26a,b,e. To a solution of 2-(1-(*tert*-butoxycarbonylamino)ethyl)-6-fluoro-3-(pyridin-2-yl)quinoline-4-carboxylic acid **25** (3.16 mmol) in DMF (10 mL) was added amine (2.0 equiv.), DIPEA (1.2 equiv.) and PyBop (2.5 equiv.) and the resulting mixture was stirred at r.t. overnight. The mixture was concentrated in vacuo and the crude residue was dissolved in EtOAc and washed with 1N NaOH, 1N HCl, water, brine, dried over sodium sulfate, filtered, and concentrated in vacuo. The crude product was purified by column chromatography on silica gel using 0-100% EtOAc/hexane as an eluent to give **26a,b,e**.

***tert*-Butyl 1-(6-fluoro-4-(methylcarbamoyl)-3-(pyridin-2-yl)quinolin-2-yl)ethylcarbamate (26a).** Obtained in 62% yield as a green solid. ^{1}H NMR (400 MHz, CD_3OD) δ ppm 8.71 (1 H, br d, *J*=4.7 Hz), 8.20 (1 H, dd, *J*=9.2, 5.3 Hz), 7.96 (1 H, td, *J*=7.8, 1.9 Hz), 7.66 (1 H, ddd, *J*=9.2, 8.4, 2.9 Hz), 7.61 (1 H, br d, *J*=8.0 Hz), 7.47 - 7.53 (2 H, m), 4.90 - 4.99 (1 H, m), 2.66 (3 H, s), 1.38 (12 H, s). Mass Spectrum (ESI) *m/z* 425.2 $[M+H]^+$.

***tert*-Butyl 1-(4-(ethylcarbamoyl)-6-fluoro-3-(pyridin-2-yl)quinolin-2-yl)ethylcarbamate (26b).** Obtained in 84% yield as a light-yellow oil. Mass Spectrum (ESI) *m/z* 439.2 $[M+H]^+$.

***tert*-Butyl 1-(4-(2-(dimethylamino)ethylcarbamoyl)-6-fluoro-3-(pyridin-2-yl)quinolin-2-yl)ethylcarbamate (26e).** Obtained in 37% yield as a yellow solid. Mass Spectrum (ESI) *m/z* 482.2 $[M+H]^+$.

Benzyl 4-(2-(1-(*tert*-butoxycarbonylamino)ethyl)-6-fluoro-3-(pyridin-2-yl)quinoline-4-carbonyl)piperazine-1-carboxylate (26d). To a solution of 2-(1-(*tert*-butoxycarbonylamino)ethyl)-6-fluoro-3-(pyridin-2-yl)quinoline-4-carboxylic acid **25** (0.15 g, 0.37 mmol) in DMF (2 mL) was added benzyl piperazine-

1-carboxylate (0.16 mL, 0.82 mmol), PyBop (429 mg, 0.82 mmol) and DIPEA (0.20 mL, 1.12 mmol) and the resulting mixture was stirred at r.t. After 1 h, the mixture was diluted with EtOAc and washed with water, brine, dried over sodium sulfate, filtered, and concentrated in vacuo. The crude product was purified by column chromatography on silica gel using 50% EtOAc/hexane to give benzyl 4-(2-(1-(*tert*-butoxycarbonylamino)ethyl)-6-fluoro-3-(pyridin-2-yl)quinoline-4-carbonyl)piperazine-1-carboxylate **26d** (55 mg, 0.09 mmol, 24% yield) as a white solid. Mass Spectrum (ESI) *m/z* 614.3 $[M+H]^+$.

Benzyl 4-(2-(1-(6-amino-5-cyanopyrimidin-4-ylamino)ethyl)-6-fluoro-3-(pyridin-2-yl)quinoline-4-carbonyl)piperazine-1-carboxylate (27). A mixture of **26d** (55 mg, 0.090 mmol) and 4N HCl in 1,4-dioxane (1 mL, 4 mmol) was stirred at r.t. After 30 min, the mixture was concentrated in vacuo to give benzyl 4-(2-(1-aminoethyl)-6-fluoro-3-(pyridin-2-yl)quinoline-4-carbonyl)piperazine-1-carboxylate. The crude product was dissolved in *n*-BuOH (1 mL). To the mixture was added 4-amino-6-chloropyrimidine-5-carbonitrile (15.2 mg, 0.1 mmol) and DIPEA (0.047 mL, 0.27 mmol) and the resulting mixture was stirred and heated to 100 °C overnight. The mixture was concentrated in vacuo. The crude product was purified by column chromatography on silica gel using 50% EtOAc/hexane as an eluent to give benzyl 4-(2-(1-(6-amino-5-cyanopyrimidin-4-ylamino)ethyl)-6-fluoro-3-(pyridin-2-yl)quinoline-4-carbonyl)piperazine-1-carboxylate **27** (56.6 mg, 0.09 mmol, quantitative). Mass Spectrum (ESI) *m/z* 632.2 $[M+H]^+$.

***tert*-Butyl 1-(4-(2-(dimethylamino)ethylcarbamoyl)-6-fluoro-3-(pyridin-2-yl)quinolin-2-yl)ethylcarbamate (26e).** Obtained in 47% yield. Mass Spectrum (ESI) *m/z* 482.2 $[M+H]^+$.

General Procedure for the Synthesis of 6a,b,e. To pure residues of **26a,b,e** (2.36 mmol) was added 4N HCl in 1,4-dioxane (8.0 mL, 32.0 mmol). The resulting mixture was stirred at r.t. for 30 min. The solvent was removed and the crude product was used without further purification. To a solution of deprotected amine in DMF (15 mL) was added 4-amino-6-chloropyrimidine-5-carbonitrile (0.364 g, 2.36 mmol) and DIPEA (1.23

mL, 7.07 mmol). The resulting mixture was heated to 95 °C for 2 h. The solvent was partially removed and the mixture was diluted with EtOAc. The mixture was washed with three time with water, brine, and dried over sodium sulfate, filtered, and concentrated in vacuo. The crude product was purified by column chromatography on silica gel using 30% [10:1 MeOH/DCM] in DCM and further purified by chiral HPLC (isopropanol/hexane gradient, AD column) to give **6a,b,e**.

2-((1*S*)-1-((6-Amino-5-cyano-4-pyrimidinyl)amino)ethyl)-6-fluoro-N-methyl-3-(2-pyridinyl)-4-quinolinecarboxamide (6a). Obtained in 36% yield as a white solid. ^{1}H NMR (400 MHz, CD_3OD) δ ppm 8.71 (1 H, d, *J*=4.3 Hz), 8.22 (1 H, dd, *J*=9.2, 5.3 Hz), 7.95 (1 H, td, *J*=7.7, 1.8 Hz), 7.91 (1 H, s), 7.69 (1 H, td, *J*=8.8, 2.7 Hz), 7.62 (1 H, d, *J*=7.8 Hz), 7.45 - 7.55 (2 H, m), 5.57 (1 H, q, *J*=6.6 Hz), 2.67 (3 H, s), 1.41 (3 H, d, *J*=6.8 Hz). Mass Spectrum (ESI) *m/z* 443.1 $[M+H]^+$. HRMS (ESI) *m/z* calculated for $C_{23}H_{19}FN_8O$ $[M+H]^+$: 443.1744; mass measured, 443.1735.

2-((1*S*)-1-((6-Amino-5-cyano-4-pyrimidinyl)amino)ethyl)-*N*-ethyl-6-fluoro-3-(2-pyridinyl)-4-quinolinecarboxamide (6b). Obtained in 42% yield as a white solid. ^{1}H NMR (400 MHz, CD_3OD) δ ppm 8.70 - 8.74 (1 H, m), 8.42 (1 H, br t, *J*=5.3 Hz), 8.21 (1 H, dd, *J*=9.3, 5.4 Hz), 7.95 (1 H, td, *J*=7.7, 1.8 Hz), 7.91 (1 H, s), 7.61 - 7.72 (2 H, m), 7.46 - 7.56 (2 H, m), 5.56 (1 H, q, *J*=6.7 Hz), 3.14 - 3.24 (2 H, m), 1.41 (3 H, d, *J*=6.7 Hz), 0.84 (3 H, t, *J*=7.2 Hz). Mass Spectrum (ESI) *m/z* 457.2 $[M+H]^+$. HRMS (ESI) *m/z* calculated for $C_{24}H_{21}FN_8O$ $[M+H]^+$: 457.1901; mass measured, 457.1909.

4-Amino-6-(1-(6-fluoro-4-(piperazine-1-carbonyl)-3-(pyridin-2-yl)quinolin-2-yl)ethylamino)pyrimidine-5-carbonitrile (6c). To a solution of benzyl 4-(2-(1-(6-amino-5-cyanopyrimidin-4-ylamino)ethyl)-6-fluoro-3-(pyridin-2-yl)quinoline-4-carbonyl)piperazine-1-carboxylate **27** (56.6 mg, 0.09 mmol) in MeOH (2 mL) was added 10% Pd/C (1.5 mg, 0.014 mmol) and the resulting mixture was stirred at r.t. under an atmosphere of hydrogen. The mixture was filtered through a celite pad. The filtrate was concentrated in vacuo to give the

crude product which was purified by preparative HPLC to give **6c** (11.6 mg, 0.023 mmol, 26% yield) as a white solid. ^{1}H NMR (400 MHz, CD_3OD) δ ppm 8.76 (1 H, dd, *J*=11.5, 4.3 Hz), 8.28 (1 H, ddd, *J*=12.7, 9.3, 5.4 Hz), 7.93 - 8.06 (2 H, m), 7.64 - 7.81 (2 H, m), 7.48 - 7.60 (2 H, m), 5.70 (1 H, dq, *J*=60.8, 6.7 Hz), 3.73 - 3.94 (2 H, m), 3.35 - 3.43 (2 H, m), 2.94 - 3.24 (2 H, m), 2.74 - 2.87 (2 H, m), 1.44 (3 H, dd, *J*=60.7, 6.7 Hz). Mass Spectrum (ESI) *m/z* 498.2 $[M+H]^+$. HRMS (ESI) *m/z* calculated for $C_{26}H_{24}FN_9O$ $[M+H]^+$: 498.2166; mass measured, 498.2172.

4-Amino-6-(1-(6-fluoro-4-(3-hydroxyazetidine-1-carbonyl)-3-(pyridin-2-yl)quinolin-2-yl)ethylamino)pyrimidine-5-carbonitrile (6d). To a solution of 2-(1-(6-amino-5-cyanopyrimidin-4-ylamino)ethyl)-6-fluoro-3-(pyridin-2-yl)quinoline-4-carboxylic acid **23** (100 mg, 0.23 mmol) in DMF (2 mL) was added azetidin-3-ol (17.0 mg, 0.23 mmol), DIPEA (0.045 mL, 0.26 mmol) and PyBOP (267 mg, 0.51 mmol) and the mixture was stirred and heated at 50 °C overnight. The mixture was cooled to r.t. and concentrated in vacuo. The crude residue was dissolved in EtOAc and washed with water, brine, dried over sodium sulfate, filtered, and concentrated in vacuo. The crude product was purified by preparative HPLC to give 4-amino-6-(1-(6-fluoro-4-(3-hydroxyazetidine-1-carbonyl)-3-(pyridin-2-yl)quinolin-2-yl)ethylamino)pyrimidine-5-carbonitrile **6d** (14.5 mg, 0.030 mmol, 13 % yield) as a white powder. ^{1}H NMR (400 MHz, DMSO-d_6) δ ppm 8.67 - 8.78 (1 H, m), 8.12 - 8.22 (1 H, m), 7.77 - 8.01 (3 H, m), 7.47 - 7.62 (3 H, m), 7.26 (1 H, br d, *J*=46.0 Hz), 5.44 - 5.80 (2 H, m), 4.06 - 4.46 (2 H, m), 3.58 - 3.96 (2 H, m), 1.15 - 1.49 (3 H, m). Mass Spectrum (ESI) *m/z* 485.2 $[M+H]^+$. HRMS (ESI) *m/z* calculated for $C_{25}H_{21}FN_8O_2$ $[M+H]^+$: 485.185; mass measured, 485.1835.

2-((1*S*)-1-((6-Amino-5-cyano-4-pyrimidinyl)amino)ethyl)-*N*-(2-(dimethylamino)ethyl)-6-fluoro-3-(2-pyridinyl)-4-quinolinecarboxamide (6e). Obtained in 63% yield as a tan solid. ^{1}H NMR (400 MHz, DMSO-d_6) δ ppm 8.78 - 8.84 (1 H, m), 8.24 (1 H, dd, *J*=9.2, 5.3 Hz), 8.17 (1 H, s), 8.09 - 8.15 (1 H, m), 7.70 - 7.80 (2 H, m), 7.60 - 7.68 (2 H, m), 5.64 (1 H, q, *J*=6.2 Hz), 3.49 - 3.63 (2 H, m), 2.99 - 3.08 (2 H, m), 2.86 (6 H, s),

1.51 (3 H, d, *J*=6.7 Hz). Mass Spectrum (ESI) *m/z* 500.2 $[M+H]^+$. HRMS (ESI) *m/z* calculated for $C_{26}H_{26}FN_9O$ $[M+H]^+$: 500.2323; mass measured, 500.2312.

2-(1-(*tert*-Butoxycarbonylamino)ethyl)-5-fluoro-3-(pyridin-2-yl)quinoline-4-carboxylic acid (28). To a solution of (*S*)-*tert*-butyl 3-oxo-4-(pyridin-2-yl)butan-2-ylcarbamate **24** (1.50 g, 5.7 mmol) in EtOH (10 mL) was added 4-fluoroindoline-2,3-dione (673 mg, 4.1 mmol) and KOH (686 mg, 12.2 mmol). The resulting mixture was heated to 95 °C overnight. The reaction mixture was allowed to cool to r.t., the solvent was partially concentrated in vacuo, and water was added. The mixture was acidified with 3 N HCl to pH 2 and extracted twice with EtOAc. The combined organic extracts was washed with water, brine, dried over sodium sulfate, filtered, and concentrated in vacuo to give 2-(1-(*tert*-butoxycarbonylamino)ethyl)-5-fluoro-3-(pyridin-2-yl)quinoline-4-carboxylic acid **28** (1.21 g, 2.94 mmol, 72% yield) as yellow foam. Mass Spectrum (ESI) *m/z* 412.2 $[M+H]^+$.

***tert*-Butyl 1-(5-fluoro-4-(methylcarbamoyl)-3-(pyridin-2-yl)quinolin-2-yl)ethylcarbamate (29).** To a solution of 2-(1-(*tert*-butoxycarbonylamino)ethyl)-5-fluoro-3-(pyridin-2-yl)quinoline-4-carboxylic acid **28** (450 mg, 1.09 mmol) in DMF (3 mL) was added methanamine (1.1 mL, 2.2 mmol), PyBop (1.71 g, 3.3 mmol) and DIPEA (0.57 mL, 3.28 mmol). The resulting mixture was stirred at r.t. overnight. The mixture was concentrated in vacuo and the crude residue was dissolved in EtOAc and washed with 1 N NaOH, 1 N HCl, water, brine, dried over sodium sulfate, filtered, and concentrated in vacuo. The crude product was purified by column chromatography on silica gel using 0-100% EtOAc/hexane as an eluent to give *tert*-butyl 1-(5-fluoro-4-(methylcarbamoyl)-3-(pyridin-2-yl)quinolin-2-yl)ethylcarbamate **29** (400 mg, 0.94 mmol, 86% yield) as a yellow solid. Mass Spectrum (ESI) *m/z* 425.2 $[M+H]^+$.

2-((1*S*)-1-((6-Amino-5-cyano-4-pyrimidinyl)amino)ethyl)-5-fluoro-*N*-methyl-3-(2-pyridinyl)-4-quinolinecarboxamide (7). To *tert*-butyl 1-(5-fluoro-4-(methylcarbamoyl)-3-(pyridin-2-yl)quinolin-2-

yl)ethylcarbamate **29** (400 mg, 0.94 mmol) was added 4 N HCl in 1,4-dioxane (1 mL, 4.00 mmol) and the resulting mixture was stirred at r.t. for 1 h. The mixture was concentrated in vacuo to give 2-(1-aminoethyl)-5-fluoro-*N*-methyl-3-(pyridin-2-yl)quinoline-4-carboxamide. The crude product was used in the subsequent step without purification.

To a solution of 2-(1-aminoethyl)-5-fluoro-*N*-methyl-3-(pyridin-2-yl)quinoline-4-carboxamide in DMF (3 mL) was added DIPEA (0.66 mL, 3.77 mmol) and 4-amino-6-chloropyrimidine-5-carbonitrile (146 mg, 0.94 mmol). The resulting mixture was heated to 90 °C for 2 h. The solvent was removed and the crude residue was purified by column chromatography on silica gel using 0-10% of [1:10 MeOH/DCM, 2 M NH_3 in MeOH]/DCM for 5 min, 20% [1:10 MeOH/DCM, 2 M NH_3 in MeOH]/DCM for 10 min, 40% [1:10 MeOH/DCM, 2 M NH_3 in MeOH]/DCM for 15 min to obtain 2-(1-(6-amino-5-cyanopyrimidin-4-ylamino)ethyl)-5-fluoro-N-methyl-3-(pyridin-2-yl)quinoline-4-carboxamide (397 mg, 0.897 mmol, 95% yield) as a yellow oil. The racemic mixture was purified by chiral HPLC (isopropanol/hexane gradient, AD column) to give 2-((1*S*)-1-((6-amino-5-cyano-4-pyrimidinyl)amino)ethyl)-5-fluoro-*N*-methyl-3-(2-pyridinyl)-4-quinolinecarboxamide **7** (0.058 g, 0.131 mmol, 14 % yield) as a white solid. ^{1}H NMR (500 MHz, DMSO-d_6) δ ppm 8.68 (1 H, dd, *J*=18.8, 4.6 Hz), 8.37 (1 H, br d, *J*=4.4 Hz), 7.80 - 8.00 (4 H, m), 7.38 - 7.60 (4 H, m), 7.28 (2 H, br d, *J*=31.1 Hz), 5.31 - 5.49 (1 H, m), 2.47 (3 H, dd, *J*=6.8, 4.6 Hz), 1.33 (3 H, br dd, *J*=35.5, 6.1 Hz). Mass Spectrum (ESI) *m/z* 443.1 $[M+H]^+$. HRMS (ESI) *m/z* calculated for $C_{23}H_{19}FN_8O$ $[M+H]^+$: 443.1744; mass measured, 443.1753.

ASSOCIATED CONTENT

Supporting Information

(i) Biological assays. (ii) Enzyme selectivity data of compounds **6a** (AM-0687) and **7** (AM-1430). (iii) Molecular formula strings and the associated biochemical and biological data. (iv) Crystal structure of PI3Kγ in complex with compound **5g**. This material is available free of charge via the Internet at http://pubs.acs.org.

Accession Code

The co-crystal structure of PI3Kγ with compound **5g** has been deposited in the protein data bank with PDB code: 5KAE.

AUTHOR INFORMATION

Corresponding Authors

* F.G.L.T.: E-mail: felix.gonzalezlopezdeturiso@biogen.com. Phone: 650-219-6176.

* Y. S.: E-mail: yshin@amgen.com. Phone: 805-313-2422.

Notes

The authors declare no competing finalcial interest. All authors are current or former employees of Amgen.

Present Addresses

†If an author's address is different than the one given in the affiliation line, this information may be included here.

ACKNOWLEDGMENT

We thank Peter Yakowec and Jin Tang for expression and purification of the PI3Kδ enzyme. We are indebted to the following people: for expert NMR elucidation, we thank David Chow and Smriti Khera, for analytical or

preparative scale chiral and chiral SFC separations, thanks go to Manuel Ventura and Brent Murphy, for procurement and large scale synthesis of certain advanced intermediates, thanks go to Yong-Jae Kim, for off-target cellular assay deployment and expertise not discussed in this report, thanks go to Sandy Ross, David Fong, and Kent Miner, for in vivo rodent pharmacokinetic study conduct, thanks go to Stacy Fide and Craig Uyeda, for useful discussions in the course of this investigation, thanks go to Robert J. Zamboni, and for fruitful discussion on the manuscript, thanks go to Christopher H. Fotsch and Margaret Chu-Moyer.

ABBREVIATIONS

AKT, (PKB) protein kinase B; Cl, clearance; CLL, chronic lymphocytic leukemia; CYP, Cytochrome P450; DCM, dichloromethane; DIPEA, *N,N*-diisopropylethylamine; DMSO, dimethyl sulfoxide; ELISA, enzyme-linked immunosorbent assay; EtOAc, ethyl acetate; FBS, FITC, fluorescein isothiocyanate; GPCR, G protein-coupled receptor; HLM, human liver microsomal; HWB, human whole blood; IgD, immunoglobulin D; IgG, immunoglobulin G; IgM, immuno-globulin M; KLH, keyhole limpet hemycin; mTOR, mammalian target of rapamycin; MeOH, methanol; PBMC, peripheral blood mononuclear cell; PBS, phosphate buffer saline; PI, phosphoinositides; PI3Ks, phosphoinositide 3-kinases; PIP2, phosphatidylinositol 4, 5- bisphosphate; PIP3, phosphatidylinositol 3, 4, 5-trisphosphate; POC, percent of control; P70S6, serine/threonine kinase target substrate is S6 ribosomal protein; RA, rheumatoid arthritis; RLM, rat liver microsomal; RTK, receptor tyrosine kinase; SEM, standard error of the mean; SFC, Supercritical Fluid Chromatography; SLL, small lymphocytic lymphoma; TFA, trifluoroacetic acid; THF, tetrahydrofuran.

REFERENCES

(1) Parker, P. J. The Ubiquitous phosphositides. *Biochem. Soc. Trans.* **2004**, *32*, 893-898.

(2) Di Paolo, G.; De Camilli, P. Phosphoinositides in cell regulation and membrane dynamics. *Nature* **2006**, *443*, 651-657.

(3) Schaeffer, E. M.; Schwartzberg, P. L. Tec family kinases in lymphocyte signaling and function. *Curr. Opin. Immunol.* **2000**, *12*, 282-288.

(4) Engelman, J. A.; Luo, J.; Canley, L. C. The evolution of phosphatidylinositol 3-kinases as regulators of growth and metabolism. *Nat. Rev. Genet.* **2006**, *7*, 606-619.

(5) Jiménez, C.; Hernández, C.; Pimentel, B.; Carrera, A. C. The p85 regulatory subunit controls sequential activation of phosphoinositide 3-kinase by Tyr kinases and Ras. *J. Biol. Chem.* **2002**, *277*, 41556-41562.

(6) Thomas, M.; Owen, C. Inhibition of PI-3 kinase for treating respiratory disease: good idea or bad idea? *Curr. Opin. Pharmacol.* **2008**, *8*, 267-274

(7) (a) Rommel, C; Camps, M.; Ji, H. PI3Kδ and PI3Kγ: partners in crime in inflammation in rheumatoid arthritis and beyond? *Nat. Rev. Immunol.* **2007**, *7,* 191-201; (b) Randis, T. M.; Puri, K. D.; Zhou, H.; Diacovo, T. G. Role of PI3Kδ and PI3Kγ in inflammatory arthritis and tissue localization of neutrophils. *Eur. J. Immunol.* **2008**, *38*, 1215-1224; (c) Ameriks, M. K.; Venable, J. D. Small molecule inhibitors of phosphoinositide 3-Kinase (PI3K) δ and γ. *Curr. Top. in Med. Chem.* **2009**, *9*, 738-753; (d) Williams, O.; Houseman, B. T.; Kunkel, E. J.; Aizenstein, B.; Hoffman, R.; Knight, Z. A.; Shokat, K. M. Discovery of dual inhibitors of the immune cell PI3Ks p110δ and p110γ: a prototype for new anti-inflammatory drugs. *Chem. Biol.* **2010**, *17*, 123-134.

(8) (a) Hennessy, B. T.; Smith, D. L.; Ram, P. T.; Lu, Y.; Mills, G. B. Exploiting the PI3K/AKT pathway for cancer drug discovery. *Nat. Rev. Drug Discov.* **2005**, *4,* 988-1004; (b) Crabbe, T.; Welham, M. J.; Ward, S. G. The PI3K inhibitor arsenal: choose your weapon! *Trends in Biochemical Sciences* **2007**, *32*, 450-456 and references therein; (c) Garcia-Echeverria, C.; Sellers, W. R. Drug discovery approaches targeting the PI3K/Akt

pathway in cancer. *Oncogene* **2008**, *27*, 5511-5526; (d) Maira, S-M; Finan, P., Garcia-Echeverria, C. From the Bench to the Bed Side: PI3K pathway inhibitors in clinical development. Phosphoinositide 3-kinase in health and disease, Volume 2, *Current Topics in Microbiology and Immunology.* Rommel, C.; Vanhaesebroeck, B.; Vogt, P. K. Eds. Springer-Verlag Berlin Heidelberg, *347*, **2011**, 209-239; (e) Wu, P.; Hu, Y. Small molecules targeting phosphoinositide 3-kinases. *Med. Chem. Comm.* **2012**, *3*, 1337-1355.

(9) Cushing, T. D.; Metz, D. P.; Whittington, D. A.; McGee, L. R. PI3Kδ and PI3Kγ as Targets for autoimmune and inflammatory diseases. *J. Med. Chem.* **2012**, *55*, 8559-8581.

(10) Yap, T. A.; Bjerke, L.; Clarke, P. A.; Workman, P. Drugging PI3K in cancer: refining targets and therapeutic strategies. *Curr. Opin. Pharmacol.* **2015**, *23*, 98-107.

(11) Fruman, D. A.; Rommel, C. PI3Kδ inhibitors in Cancer: rationale and serendipity merge in the clinic. *Cancer Disc.* **2011***, 7,* 562-572.

(12) Awan, F. T.; Byrd, J. C. New strategies in chronic lymphocytic leukemia: shifting treatment paradigms. *Clinical Cancer Research.* **2014**, *20*, 5869-5874.

(13) Idelalisib (Zidelig) is intended to be used in patients who have received at least two prior systemic therapies.

(14) (a) Shin, Y.; Suchomel, J.; Cardozo, M.; Duquette, J.; He, X.; Henne, K.; Hu, Y.-L.; Kelly, R C.; McCarter, J.; McGee, L. R.; Medina, J. C.; Metz, D.; San Miguel, T.; Mohn, D.; Tran, T.; Vissinga, C.; Wong, S.; Wannberg, S.; Whittington, D. A.; Whoriskey, J.; Yu, G.; Zalameda, L.; Zhang, X.; Cushing, T. D. Discovery, optimization, and in vivo evaluation of benzimidazole derivatives AM-8508 and AM-9635 as potent and selective PI3Kδ inhibitors. *J. Med. Chem.* **2016**, *59*, 431-447; (b) Gonzalez-Lopez de Turiso, F.; Shin, Y.; Brown, M.; Cardozo, M.; Chen, Y.; Fong, D.; Hao, X.; He, X.; Henne, K.; Hu, Y.-L.; Johnson, M. G.; Kohn, T.; Lohman, J.; McBride, H. J.; McGee, L. R.; Medina, J. C.; Metz, D.; Miner, K.; Mohn, D.; Pattaropong, V.;

Seganish, J.; Simard, J. L.; Wannberg, S.; Whittington, D. A.; Yu, G.; Cushing, T. D. Discovery and in vivo evaluation of dual PI3Kβ/δ inhibitors. *J. Med. Chem.* **2012**, *55*, 7667-7685 (c) D'Angelo, N. D.; Kim, T.-S.; Andrews, K.; Booker, S. K.; Caenepeel, S.; Chen, K.; D'Amico, D.; Freeman, D.; Jiang, J.; Liu, L.; McCarter, J. D.; San Miguel, T.; Mullady, E. L.; Schrag, M.; Subramanian, R.; Tang, J.; Wahl, R. C.; Wang, L.; Whittington, D. A.; Wu, T.; Xi, N.; Xu, Y.; Yakowec, P.; Yang, K.; Zalameda, L. P.; Zhang, N.; Hughes, P.; Norman, M. H. Discovery and optimization of a series of benzothiazole phosphoinositide 3-Kinase (PI3K)/mammalian target of rapamycin (mTOR) dual inhibitors. *J. Med. Chem.* **2011**, *54*, 1789-1811; (d) Nishimura, N.; Siegmund, A.; Liu, L.; Yang, K.; Bryan, M. C.; Andrews, K. L.; Bo, Y.; Booker, S. K.; Caenepeel, S.; Freeman, D.; Liao, H.; McCarter, J.; Mullady, E. L.; San Miguel, T.; Subramanian, R.; Tamayo, N.; Wang, L.; Whittington, D. A.; Zalameda, L.; Zhang, N.; Hughes, P. E.; Norman, M. H. Phospshoinositide 3-kinase (PI3K)/mammalian target of rapamycin (mTOR) dual inhibitors: discovery and structure-activity relationships of a series of quinoline and quinoxaline derivatives. *J. Med. Chem.* **2011**, *54*, 4735-4751; (e) Stec, M. M.; Andrews, K. L.; Booker, S. K.; Caenepeel, S.; Freeman, D. J.; Jiang, J.; Liao, H.; McCarter, J.; Mulladi, E. L.; San Miguel, T.; Subramanian, R.; Tamayo, N.; Wang, L.; Yang, K.; Zalameda, L. P.; Zhang, N.; Hugues, P.; Norman, M. H. Structure–activity relationships of phosphoinositide 3-kinase (PI3K)/mammalian target of Rapamycin (mTOR) dual inhibitors: investigations of various 6,5-heterocycles to improve metabolic stability. *J. Med. Chem.* **2011**, *54*, 5174-5184.

(15) Cushing, T. D.; Hao, X.; Shin, Y.; Andrews, K.; Brown, M.; Cardozo, M.; Chen, Y.; Duquette, J.; Fisher, B.; Gonzalez-Lopez de Turiso, F.; He, X.; Henne, K. R.; Hu, Y.-L.; Hungate, R.; Johnson, M. G.; Kelly, R. C.; Lucas, B.; McCarter, J. D.; McGee, L. R.; Medina, J. C.; San Miguel, T.; Mohn, D.; Pattaropong, V.; Pettus, L. H.; Reichelt, A.; Rzasa, R. M.; Seganish, J.; Tasker, A. S.; Wahl, R. C.; Wannberg, S.; Whittington, D. A.; Whoriskey, J.; Yu, G.; Zalameda, L.; Zhang, D.; Metz, D. P. Discovery and in vivo evaluation of (*S*)-*N*-(1-(7-

fluoro-2-(pyridin-2-yl)quinolin-3-yl)ethyl)-9*H*-purin-6-amine (AMG 319) and related PI3Kδ inhibitors for inflammation and autoimmune disease. *J. Med. Chem.* **2015**, *58*, 480-511.

(16) (a) Cushing, T. D.; Gonzalez-Lopez de Turiso, F.; Hao, X.; Shin, Y. Heterocyclic compounds and their uses. PCT Int. Appl. WO 2011075628 A1, June 23, **2011**; (b) Chen, Y.; Cushing, T. D.; Fisher, B.; Gonzalez-Lopez de Turiso, F.; Hao, X.; Shin. Y. Heterocyclic compounds and their uses. PCT Int. Appl. WO 2012087784 A1, June 26, **2012**.

(17) Cushing, T. D.; Hao, X.; Lohman, J. W.; Shin, Y. Heterocyclic compounds and their uses. PCT. Int. Appl. WO 2010151735 A2, December, 29, **2010**.

(18) Lucas, B. Heterocyclic compounds and their use as inhibitors of PI3K activity. PCT. Int. Appl. WO 2012003262 A1, January, 5, **2012**.

(19) (a) Bui, M. H. T.; Fisher, B.; Hao, X.; Lucas, B. Heterocyclic compounds and their use as inhibitors of PI3K activity. PCT Int. Appl. WO 2012003274 A1, January, 5, **2012**; (b) Cushing, T. D.; Lohman, J. W.; Shin, Y. Quinoline derivatives as PIK3 inhibitors. PCT Int. Appl. WO 2012068343 A1, May 24, **2012**.

(20) Bui, M.; Hao, X.; Shin, Y.; Cardozo, M.; He, X.; Henne, K.; Suchomel, J.; McCarter, J.; McGee, L. R.; San Miguel, T.; Medina, J. C.; Mohn, D.; Tran, T.; Wannberg, S.; Wong, J.; Wong, S.; Zalameda, L.; Metz, D.; Cushing, T. D. Synthesis and SAR study of potent and selective PI3Kδ inhibitors. *Bioorg. Med. Chem. Lett.* **2015**, *25*, 1104-1109.

(21) Laurence, C.; Brameld, K. A.; Graton, J.; Le Queste, J.-Y.; Renault, E. The pK_{BHX} database: toward better understanding of hydrogen-bond basicity for medicinal chemists. *J. Med. Chem.* **2009**, *52*, 4073-4086.

(22) Pfitzinger, W. Chinolinderivate aus isatinsäure. *J. Prakt. Chem*. **1886**, *33*, 100.

(23) This result contrasts with the observation from Patel, L. and co-workers (*J. Med. Chem.* **2016** ASAP, DOI: 10.1021/acsjmedchem.6b00213) on which the microsomal stability of related cyano-aminopyrimidine-containing PI3K inhibitors was not a good predictor of in vivo clearance.

(24) See supporting information for kinase selectivity profile for these analogs.

(25) Bissantz, C.; Kuhn, B.; Stahl, M. A Medicinal chemist's guide to molecular interactions. *J. Med. Chem.* **2010**, *53*, 5061-5084.

(26) In this assay, the murine B cell-transgenic line 3751, which has only surface-bound IgM and lacks secreted/circulating IgM was employed ($IgM_{membrane}$ only; IgM_m). These transgenic mice were used to avoid IgM/anti-IgM immune complex formation that could promote serum sickness in normal mice. See also: Boes, M.; Esau, C.; Fischer, M. B.; Schmidt, T.; Carroll, M.; Chen, J. Enhanced B-1 cell development, but impaired IgG antibody responses in mice deficient in secreted IgM. *J. Immunol.* **1998,** *160*, 4776-4787.

Table of Contents Graphic

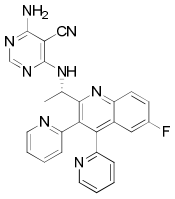

4

Cellular potency
pAKT IC_{50} = 8.6 nM

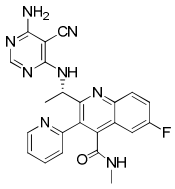

6a

Cellular potency
pAKT IC_{50} = 0.7 nM
HWB,u (pAKT) IC_{50} = 4.6 nM
Rat KLH
IgG ED_{50} = 0.026 mg/kg
IgM ED_{50} = 0.016 mg/kg
Rat PK
Clu = 2.3 L/hr/kg

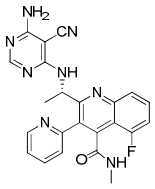

7

Cellular potency
pAKT IC_{50} = 0.8 nM
HWB,u (pAKT) IC_{50} = 7.7 nM
Rat KLH
IgG ED_{50} = 0.016 mg/kg
IgM ED_{50} = 0.015 mg/kg
Rat PK
Clu = 1.7 L/hr/kg